# Investigation of Breast Cancer in Fabricated Breast Phantom Using Wearable Patch Antenna

**Aylin Zurnacı**

Submitted to the
Institute of Graduate Studies and Research
in partial fulfillment of the requirements for the degree of

Master of Science
in
Electrical and Electronic Engineering

Eastern Mediterranean University
February 2023
Gazimağusa, North Cyprus

Approval of the Institute of Graduate Studies and Research

Prof. Dr. Ali Hakan Ulusoy
Director

I certify that this thesis satisfies all the requirements as a thesis for the degree of Master of Science in Electrical and Electronic Engineering.

Assoc. Prof. Dr. Rasime Uyguroğlu
Chair, Department of Electrical and Electronic Engineering

We certify that we have read this thesis and that in our opinion it is fully adequate in scope and quality as a thesis for the degree of Master of Science in Electrical and Electronic Engineering.

Asst. Prof. Dr. Ali Işın
Co-Supervisor

Assoc. Prof. Dr. Rasime Uyguroğlu
Supervisor

Examining Committee

1. Prof. Dr. Mehmet Kuşaf

2. Prof. Dr. Şener Uysal

3. Assoc. Prof. Dr. Rasime Uyguroğlu

# ABSTRACT

In this study, a wearable microstrip patch antenna design is proposed to detect breast cancer based on the contrast in dielectric properties between healthy and infected (malignant) tissues. To test the proposed antenna, a three layered (skin, fat, glandular) breast phantom that can mimic human breast has been developed. A wearable, small size printed patch antenna was used on breast phantom for the stage I and stage II cancer detection. Return loss values of a 28.8 × 28.8 $mm^2$ patch antenna which implemented on FR4 structure were used to study effect of the tumor. Firstly, a multilayer breast phantom model was designed by using CST Microwave Studio and simulations were taken to detect the tumor. Additionally, a realistic breast phantom composed of skin, fat and glandular was fabricated to test the designed antenna. After carrying out the simulations, the realistic healthy and infected breast phantoms were obtained and the aforementioned antenna was fabricated. The return loss measurements were taken on fabricated phantoms by a network analyzer (NanoVNA-F Network Analyzer) and compared with the simulated results. Measurement of fabricated breast phantoms are in good agreement with the simulated results.

The proposed study can be considered as a promising method for breast cancer research and presents a new and promising method to doctors in the detection of breast cancer with the obtained antenna and sheds light on the researchers with the fabricated breast phantom.

**Keywords:** Breast cancer detection, Microwave imaging, Tissue phantoms, Biomedical, Wearable antenna

# ÖZ

Bu çalışmada, meme fantomunda evre I ve evre II kanser tespiti için giyilebilir, küçük boyutlu baskılı yama anten kullanılmıştır. FR4 yapısı üzerine uygulanan 28.8 x 28.8 $mm^2$ yama antenin geri dönüş kaybı değerleri, sağlıklı ve tümörlü meme dokularının etkisini incelemek için kullanıldı. Öncelikle CST Microwave Studio kullanılarak çok katmanlı bir meme fantom modeli tasarlanmış ve tümörün teşhisi için simülasyonlar alınmıştır. Ek olarak, tasarlanan anteni test etmek için deri, yağ ve salgı bezlerinden oluşan gerçekçi bir meme fantomu üretildi. Simülasyonlar alındıktan ve gerçekçi sağlıklı ve tümörlü meme fantomu üretildikten sonra, anten imal üretildi ve fabrikasyon fantomlar üzerinde bir ağ analiz cihazı (NanoVNA-F V2 Vector Network Analyzer) ile geri dönüş kaybı ölçümleri alındı.

CST Microwave Studio ile elde edilen sağlıklı ve enfekte meme modellerinin simülasyonları, ölçülen sonuçlarla iyi bir uyum içinde olduğu gözlemlendi.

Önerilen çalışmanın meme kanseri çalışmaları için umut verici bir yöntem olduğu gösterilmiştir. Tümör tespitinde yeni ve umut vadeden bir yöntemi doktorlara sunmakla birlikte elde edilen fantom ile araştırmacılara da ışık tutuyor.

**Anahtar Kelimeler:** Meme kanseri teşhisi, Mikrodalga görüntüleme, Doku fantomları, Biyomedikal, Giyilebilir anten.

# ACKNOWLEDGEMENT

Foremost, I would like to express my sincere gratitude to my supervisors Assoc. Prof. Dr. Rasime Uyguroğlu and Assist.Prof. Dr. Ali Işın for their continuous support, patience, motivation and immense knowledge. Nothing of this could be achieved without their help and support. I'm extremely grateful to Dr Wael Ali Zeinelabedeen Elwaseef Mohamed who allowed me to use his device to take measurements and patiently helped complete my measurements.

I also would like to thank my fiancée, my mother, and my friends who always supported me.

# TABLE OF CONTENTS

# LIST OF TABLES

# LIST OF FIGURES

# LIST OF SYMBOLS AND ABBREVIATIONS

| | |
|---|---|
| B | Magnetic field flux density |
| $C_o$ | The speed light in free space |
| E | Electric field intensity vector |
| $F_r$ | Resonant frequencies |
| G | Conductance |
| H | Magnetic field intensity vector |
| $L_{eff}$ | Effective length |
| $P_{rad}$ | Radiated power |
| Rr | Radiation impedance |
| Y | Complex propagation constant |
| $\delta_{eff}$ | Effective loss tangent |
| $\varepsilon$ | Permittivity |
| $\varepsilon_r$ | Relative permittivity |
| $\eta$ | Wave impedance |
| $\lambda$ | Wavelength |
| $\mu$ | Relative permeability |
| $\sigma$ | Electric conductivity |
| $\Omega$ | Ohm |
| BAN | Body Area Network |
| BW | Bandwidth |
| CST | Computer Simulation Technology |
| EIRP | Equivalent Isotopically Radiated Power |

| | |
|---|---|
| EM | Electromagnetic |
| EMC | Electromagnetic Compatibility |
| EMI | Electromagnetic Interference |
| ERP | Equivalent Radiated Power |
| FR 4 | Flame Retardant 4 |
| HBC | Human Body Communication |
| HF | High Frequency |
| IBC | Intra Body Communication |
| IEEE | Institute of Electrical and Electronic Engineers |
| IMD | Implantable Medical Devises |
| ISM | Industrial Scientific and Medical |
| MICS | Medical Implants Communication System |
| PIFA | Planar Inverted F Antenna |
| RF | Radio Frequency |
| RMS | Rood Mean Square |
| SAR | Specific Absorption Rate |
| SIW | Substrate Integrated Waveguide |
| UWB | Ultra Wide Band |
| WBAN | Wireless Body Area Network |
| WHO | World Health Organization |

# Chapter 1

# INTRODUCTION

Prostate, lung and breast tumors are the most common types of solid tumor cancers in the world. Although all types of cancer develop in one region and then can spread to other regions, they are named according to the region where they occur. Breast cancer is a cancer type that starts in breast cells and can spread through lymph nodes and even to bone, liver and lung. According to World Health Organization, in 2020, 2.3 million cancer cases and 685,000 deaths were occurred in the world. In line with this information, there are many studies emphasizing the importance of early detection in breast cancer [1-2]. The X-ray mammography is a current standard for early breast cancer detection in clinical applications. Although x-ray mammography uses low doses and can produce high resolution images, many of its limitations have been documented [3]. Although there is an excess research examining the advantages of imaging methods used in breast cancer detection, a search for new imaging techniques has arisen, especially because of the presence of x-rays and the possibility that cancer cells formed in women with dense breasts may be missed by x-ray mammography. Microwave imaging is the one of the most promising techniques for breast cancer detection. There are many research studies for early breast cancer detection by using microwave antennas. Jahan et al., [4] proposed a microstrip patch antenna design with semi-circular and rectangular cutting slots to detect the tumor in breast phantom by variation of S11 and SAR analysis using CST Microwave Studio. In another study, it is suggested that the breast tumor location can be found by using scattering parameters

by a 1x8 array of micro strip phased array antennas operating at 2.4 GHz [5]. Nagia Ali et al., [6] are proposed an antenna for detecting breast cancer in stage II.

Although every country has medical device production and clinical research regulations, changes can be observed in some substances of these regulations according to the countries. All over the world, as a result of clinical research, in order for a device to be put into production and used in the clinic, it must go through many steps and be approved by certain tests. In order to test the accuracy of biomedical devices on humans, it is necessary to obtain approved reports from the ethics committee. After the approval, volunteers who can address the use of the device should be found and then devices can be used on these volunteers to optimize, test and develop the researched devices. While developing antennas, there may be differences between the values obtained in the computer environment and the actual values due to many factors such as laboratory environment and production, and modifications may be required in the antenna design to achieve good matching. For this reason, tissue mimic phantoms are developed to test and optimize biomedical antennas before using antennas on real human body [7]. Kumar et al., [8] proposed a study for breast cancer detection by using micro strip patch antenna array on fabricated single layer breast phantom that can mimic skin, fat and tumor. Moreover, Vivaldi Antenna (BSAVA) sensor is proposed for breast cancer detection on fabricated homogenous one-layer breast phantom that can mimic skin, fat, muscle and tumor [9]. In this thesis, a wearable microstrip patch antenna design is proposed to detect breast cancer based on the contrast in dielectric properties between healthy and infected (malignant) tissues. To test the proposed antenna, a three layered (skin, fat, glandular) breast phantom that can mimic human breast has been developed.

## 1.1 Thesis Objective

The objective of this thesis is to improve a scenario for detection of breast cancer depending on dielectric differences between healthy and malignant tissues. This thesis was completed in two stages. The first stage includes the antenna design and the simulations of the antenna on the breast phantom by using CST Microwave Studio, and the second stage includes the realistic breast phantom design in order to test the designed antenna. A wearable, small size printed patch antenna is used on breast phantom for the stage I and stage II cancer detection. 28.8×28.8 $mm^2$ patch antenna which implemented on FR4 structure with 1.6 mm thickness and relative permittivity 4.3 has been designed and fed with a 50 ohm microstrip line with 3.05 width by using CST Microwave Studio.

## 1.2 Thesis Contribution

In this study, an antenna is proposed to be used for further investigation by specialist to detect breast cancer stages depending upon the tumor size and location. The breast model is designed according to dielectric parameters (σ, μ, Ɛ) of human breast at ISM frequency.

The following achievements can be listed as a thesis contribution,

a) Designing and simulating a micro strip patch antenna for breast cancer detection.

b) Designing a 3 layered realistic breast phantom, which have dielectric properties close to the breast tissues and physically close to real breast.

c) Implementing antenna on realistic human breast phantom.

d)Using antenna return loss parameters to differentiate healthy breast from tumorous breast.

# Chapter 2

# OUTLINE ON BIOMEDICAL APPLICATION

## 2.1 Introduction

Biomedical engineering is a multidisciplinary field which has an important role in detection, treatment and even in following up the patient status in the hospital. Today, in medical applications many diagnostic and treatment methods have been developed and different methods continue to be developed day by day. Among these methods, antennas are one of the methods used and being investigated in many detection and treatment of various diseases. Microwave imaging, pacemakers, deep neural implants, microwave antennas for thermal ablation, magnetic resonance imaging and endoscopy are some methods developed using biomedical antennas [10].

## 2.2 Type of Antennas Used in Biomedical Applications

The application of antennas in the biomedical field is grouped under 3 main headings: Data transfer, detection and treatment. As shown in Figure 1, each of the main heading applications includes different antennas. Data transfer application which is called biomedical telemetry can be carried out by ingestible antennas, wearable antennas and implantable antennas. Antennas for MRI and antennas for microwave imaging are the antennas that used in detection and on the other hand, the thermal ablation antennas are the one that used for treatment of some diseases [10].

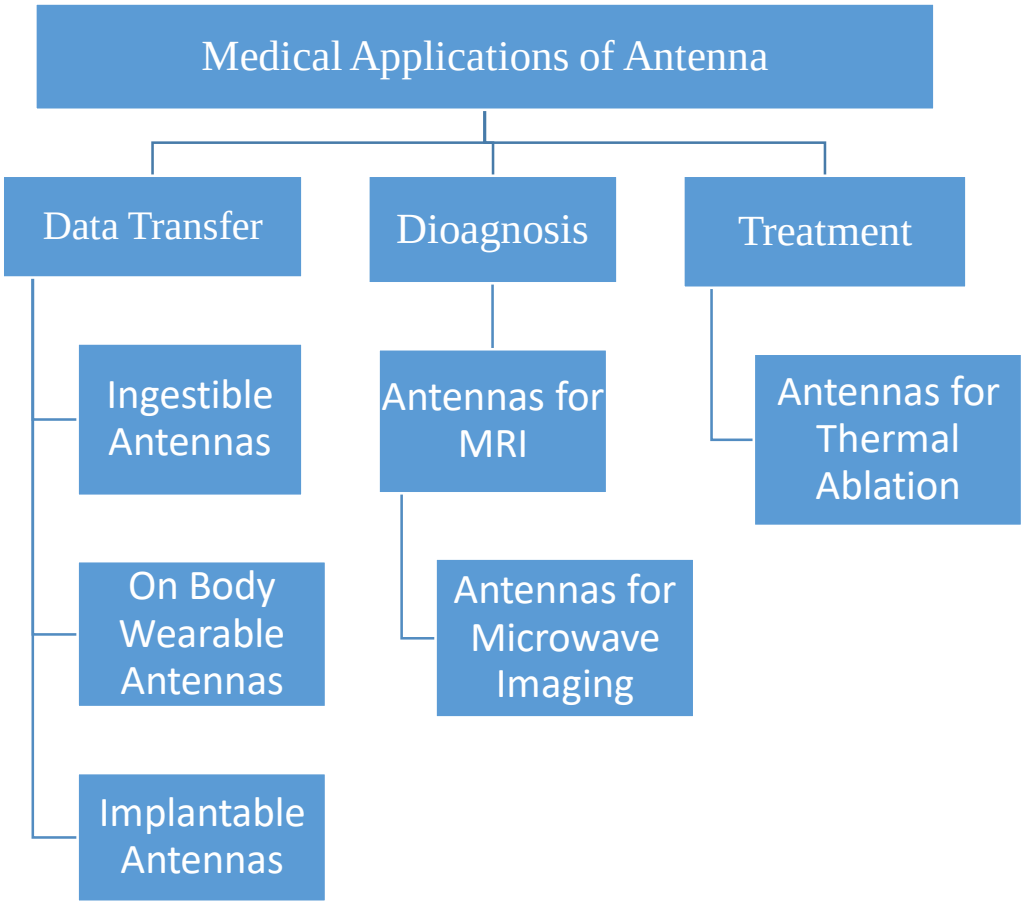


Figure 1: Group of antennas used in Biomedical applications

### 2.2.1 Data Transformation

#### 2.2.1.1 Ingestible Antennas

Ingestible antennas are the name given to the antennas used in the capsule endoscopy method. Capsule endoscopy method is used to transmitted data from inside of the body to the outside. Capsule antennas consist of antenna, camera and battery. Capsule antennas are used for detection of diseases such as Crohn disease, tumorous cancers and celiac disease by transmitting video signals to the receiver with the help of a camera while passing through the digestive system [11].

Ingestible antennas are generally designed as conformal, with wide impedance bandwidth, and orientation matching is important [10]. There are different antenna

design studies for capsule endoscopy in the literature. Lee et al., [12] designed a spiral shaped antenna which operates at 500 MHz. Hatmiet al., [13] designed two spiral coils which operate at 40 MHz. One of the coils is designed as transmitter and the other is designed as receiver coil placed on body. On the other hand, Liu et al., [14] designed a circular polarized helical shaped antenna.

#### 2.2.1.2 On Body Wearable Antennas

Wearable antennas are used to measure parameters such as the patient's heart rate, oxygen level and temperature over the body. To measure these parameters on the body, antennas designed with wide band and low reflection coefficient. In addition, high gain and efficiency are the parameters to be considered when designing wearable antennas [10]. There are different antenna designs in the literature for wearable technology. For example, Hong et al., [15] and Agneessens et al., [16] designed substrate integrated waveguide. Based on SIW technology Hong et al used shorting pins and full ground plane and Agneessens et al., used shorting wall in their wearable antenna studies. In addition to SIW technology as another wearable technology Ashyap et al., [17] designed u-shaped jean fabric patch antenna that can operate at 2.45 GHz. On the other hand, Al-Ghamdi et al., [18] showed that a three-layer dipole structure is promising for wearable antenna technology.

#### 2.2.1.3 Implantable Antennas

Implantable antennas are generally designed for continuous health monitoring, such as brain activity monitoring or glucose level measurements, as well as for detecting a tumor. In the literature, implantable antennas designed as planar antenna, wire antenna, conformal antenna, spiral antenna, slot antenna and planar inverted f antenna (PIFA). Implantable antennas are generally small, biocompatible, and designed according to SAR standards for patient safety [19].

The implantable antenna study on biotelemetry of Karacolak et al., [20] can be given as an example of the studies for implantable antenna. It is seen that Karacolak et al., have developed an implantable dual band antenna to monitor glucose, temperature and physiology parameters from a wireless distance and tested it on animals. Since the biocompatibility of the implantable antennas is a factor to be considered, while designing the antenna they paid attention to operate in the appropriate range for the Medical Implant Communication Service band (402 MHz-405 MHz) and Industrial Scientific and Medical band (ISM Band 2.4 GHz-2.8 GHz).

### 2.2.2 Detection

#### 2.2.2.1 Antennas for MRI

MRI is the most important method used today to obtain high-resolution images of the body in order to examine the tissue, organ and skeletal system of patients and to diagnose various diseases. Radio frequency receiving and transmitting antennas are involved during magnetic resonant imaging. The task of the transmitting antennas is to emit electromagnetic pulses to the human body, and the task of the receiving antennas is to detect the RF signals emitted from the human body to create image of the body [21]. In the literature, there are many studies to improve antenna design performance for MRI systems. Imran et al., [22] conducted a study to reduce the antenna size and design a high-performance antenna for MRI. In this study, a cylindrical patch antenna was designed to operate in the UWB spectrum from 7.8 GHz to 15 GHz. The electromagnetic information coming from the body tissue, which is the duty of the receiving antenna, was determined from the S-parameter values of the designed antenna.

#### 2.2.2.2 Antennas for Microwave Imaging

Microwave imaging technology is a method based on detecting tumorous tissues. Since tumor tissues have higher dielectric properties than healthy tissues, Microwave imaging technology is based on detection of cancerous cells depending on the dielectric difference of tumor and healthy tissues. Although there are many imaging techniques that are actively used in the clinic today, many of them are considered harmful because they scatter X-rays. Therefore, as a result of the studies in the literature, microwave imaging is accepted as a promising technology for medical imaging due to its low power, low cost and non-ionizing properties [10].

As mentioned above, cancer detection with microwave imaging is made according to the electrical contrast of normal tissue and cancerous tissues. Depending on this principle, Microwave energy is transmitted from the transmitter to the organ where the tumor is detected by the receiver for tumor detection. Reflection in normal tissue is less and reflection in microwaves passing through tumor tissue is higher and this causes a change in electrical properties. According to the obtained reflection coefficient values, an image is created using various signal processing techniques [23-24].

Jamlos et al., [25] has designed UWB array antenna which can operate from 2.6 GHz to 13.1 GHz for brain tumor detection according to scattering parameters. In their study, they analyzed the S-parameter changes according to the presence and absence of the tumor in a skull model. As a result of the study, lower reflection coefficient values were obtained in the tumor skull model compared to the tumor-free model. On the other hand, Gagandeep and Annapreet [26] have studies in the field of breast microwave imaging for tumor detection. They developed their study based on

monostatic radar-based approach to microwave imaging. According to this technique, they designed a cubic shaped resonator antenna operating at 8.3 GHz. The antenna was designed using the FR-4 substrate. After the antenna was designed and printed, they obtained a breast phantom that could mimic the real breast under the microwave frequencies. They designed the whole artificial phantom with gelatin to mimic skin, petroleum jelly to mimic fat, and wheat flour to mimic the tumor. After the phantom design, they took measurements when the antenna was at a distance of 5 mm on the breast phantom. According to the measurements obtained from tumor and non-tumor structures, they determined that the return loss value of the tumor structure was higher than that of the healthy structure. Finally, they processed all the results and obtained a 2D image using Matlab.

Moreover, Islam et al., [9] have designed Vivaldi antenna which can be operate at 3.01 to 11 GHz. They designed the antenna for breast tumor detection and they tested on a realistic homogenous single layer breast phantom. They used two antennas on the breast model and achieved that microwave antenna was suitable for breast imaging. On the other hand, Nagia Ali et al., [27] have designed an implantable patch antenna that can operate on ISM band and they took measurements on the real human breast. They concluded that when the tumor radius increases it effects the resonant frequency and the return loss.

### 2.2.3 Treatment

#### 2.2.3.1 Antennas for Microwave Ablation

Nowadays, the use of antennas under the thermal ablation method is quite common in the treatment of cancer diseases. Thermal ablation method has established its place in a clinic, especially since it is minimally invasive and allows difficult-to-reach tumor

tissues to be treated under imaging [28]. Studies have shown that the use of microwave antennas extends patient life by 33-57% for another 5 years [29]. Under the name of thermal ablation, Radio Frequency Ablation (RFA) and Microwave Ablation (MWA) are two treatments used in the clinic. The thermal ablation process is usually performed with the aid of an ultrasound and is designed using the difference in thermal sensitivity between normal tissue and tumorous tissue. Radio frequency ablation transmits energy by creating an electromagnetic field at a frequency of 460-550 kHz. The transmitted energy creates a temperature of 1000 C and destroys the tumor within 15 minutes [30]. On the other hand, microwave ablation generates heat using microwave frequencies between 300 MHz and 300 GHz and has been accepted as a more advantageous new method than RFA. [31-32] Since thermal ablation is a minimally invasive procedure and requires injection into the tumor, antennas should be designed interstitial coaxial as long needle. There are designs such as monopole, dipole, slot and choke in the literature [10].

In the Turkish Republic of Northern Cyprus Nalbantoğlu state hospital, the interventional radiology doctors use the thermal ablation process in the treatment of tumor tissues. Although radiofrequency therapy has been used for many years in the past, microwave ablation method is preferred in ablation procedures, especially because of its short duration, and I personally provide clinical support. Medtronic Emprint product is used for MWA process. Covidien brand Emprint model ablation system is a system based on thermosphere technology and is used for tumor ablation in the treatment of liver and lung tumors. In this system, the electromagnetic field is

transmitted to the target tissue by the antenna mounted on the probe [33]. The design of the product is shown in Figure 2 [34].

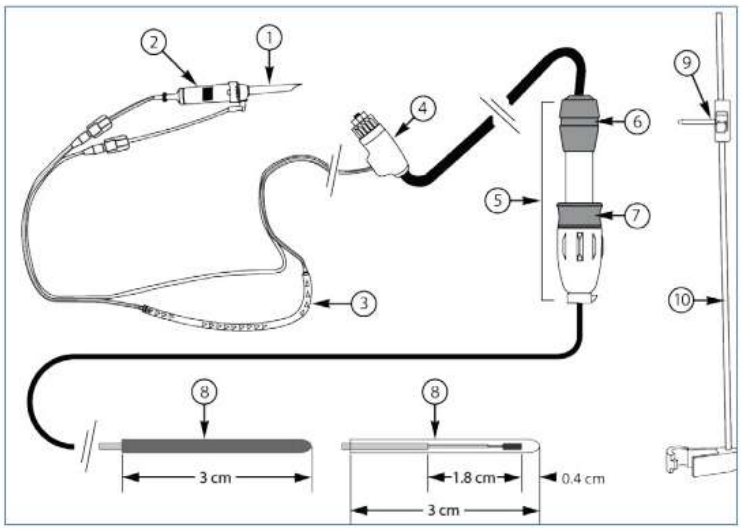


Figure 2: Emprint Ablation catheter.
(1) Intravenous IV Bag Spike; (2) Drip Chamber; (3) Pump Tubing; (4) Generator Connector; (5) Ablation Catheter Handle; (6) Top Groove, (7) Control Ring, (8) Radiating Section; (9) Clip; (10) Rail

## 2.3 Frequency Band of Biomedical Antennas

The Medical Implant Communication Service (MICS) Band and The Industrial, Scientific and Medical (ISM) Band are the two most common standards used as frequency bands in biomedical antenna studies.

### 2.3.1 The Medical Implant Communication Service (MICS) Standard

MICS is a mobile radio service for implantable devices used in detection or therapy such as pacemakers. It is a low-power standard based on the 402-405 MHz frequency band. Devices designed in accordance with the MIC standard are connected to the external control unit and the changes in the parameters are observed from the control unit. This system is considered suitable for use in implantable devices, as

electromagnetic signals at 402-405 MHz frequencies can easily spread to the human body [35].

### 2.3.2 The Industrial, Scientific and Medical (ISM) Band Standard

The ISM band is a band that operates between 2.4 GHz and 2.4835 GHz and is used in the design of wifi-bluetooth, cordless phones and household microwave ovens, and is also suitable for use in medical device designs. Systems designed in accordance with this standard should be designed with the spread spectrum [36].

# Chapter 3

# OUTLINE ON BREAST TUMOR

## 3.1 Introduction

There are many types of cancer, categorized as hematology and solid tumor cancers. Cancers can develop in one part of the body and then spread to different regions and are named according to the region where they started. Hematological cancers are cancer types related to blood cells, and tumor cancers are cancer types that occur in body organs and tissues. Prostate, lung and breast tumors are the most common types of solid tumor cancers in the world. Breast cancer is a type of cancer that starts in breast cells and can spread to lymph nodes, bone, liver and lungs.

The World Health Organization announced that 2.3 million breast cancer cases and 685,000 deaths occurred in the world in 2020. The Figure 3 shows the breast cancer distribution by country. Arnold et al., [1] conducted a study using the values published by the World Health Organization regarding to breast cancer cases in 2020, and in their study, they predicted that new cancer cases will exceed 3 million in 2040 and the number of deaths will reach 1 million.

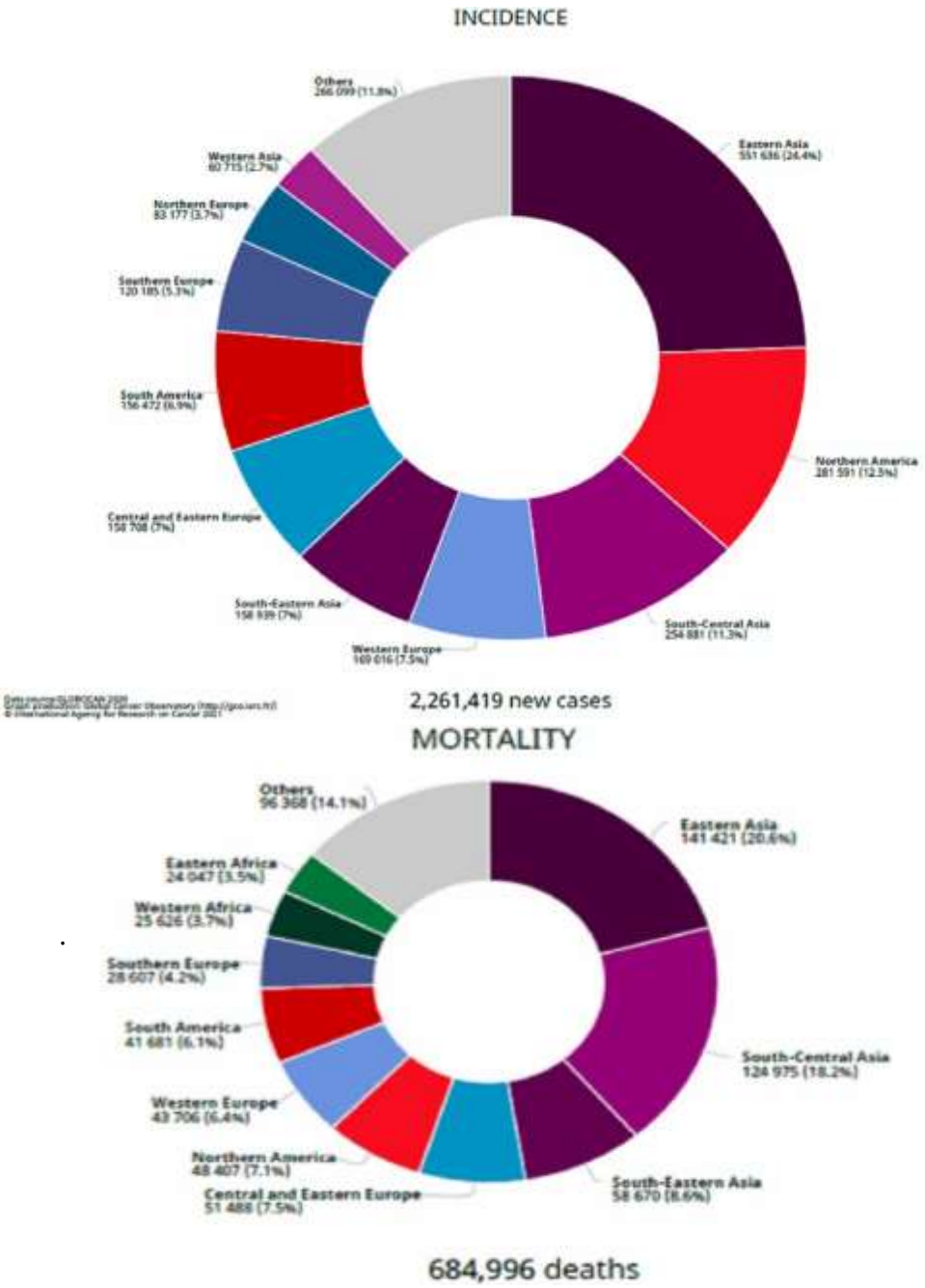


Figure 3: Breast cancer distribution by countries in 2020 [1].

In many studies, it is emphasized that early detection of breast cancer is important and a decrease in mortality rate is observed with early detection [2]. In the clinic applications mammography, ultrasound and MRI devices are used for breast cancer detection. Today, mammography is the most widely used method for diagnosing breast cancer. However, despite the fact that mammography is the most widely used

method in breast cancer detection, according to the literature it is not a 100% advantageous method since it includes ionization radiation and can give false negative and false positive results in women with dense breasts [37-38].

## 3.2 Breast Tumor Stages

Cancerous cells divide and multiply in order to stay in the body, and by creating abnormal cells, they form tumors in the body. There are two types of cancer cells: Benign and Malignant, that is, noncancerous and cancerous tumors. Benign cancers consist of cells that look like normal cells, grow slowly and do not spread to different tissues of the body. Malignant cancers are the opposite of benign and consist of cells that can spread to other tissues of the body unless controlled. As mentioned in the introduction part, breast cancers usually start from the nipple or mammary glands and spread to other parts of the body. Breast cancers are examined in 5 different stages, starting from stage 0 to stage 4. Breast cancer stages are grouped according to the size and spread of the tumor. Tumors smaller than 2 cm are considered stage 1, tumors between 2 and 5 cm are considered stage 2, and tumors larger than 5 cm are generally considered stage 3. In Stage 4, the tumor has spread to other organs. The tumor locations in the stages are shown in the Figure 4 [39-40].

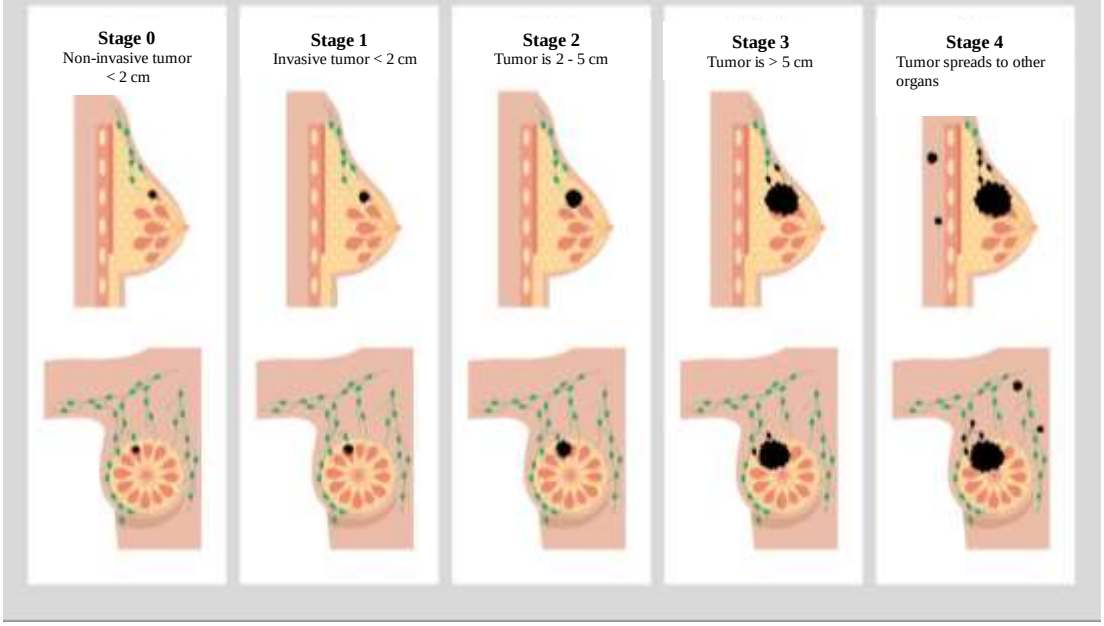


Figure 4: Breast cancer stages

## 3.3 Tissue Mimic Phantoms

Tissue mimic phantoms and human body phantoms are structures designed to mimic human body tissues. Especially in microwave imaging studies, the use of phantoms is common during antenna design and measurement. These structures, which play an important role in the design and development of systems, need to be designed to mimic tissue and its 3-dimensional structure. Although microwave systems are usually modeled and simulated with the help of a program, during the initial design, development, performance and calibration of the antennas, since they do not reflect the real parameters due to environmental, electrical and similar reasons; It is more appropriate to use tissue mimic phantoms in clinical trials instead of testing antennas on real people [7]. In microwave systems, phantoms are examined in two categories: 1- Theoretical phantoms and Voxel phantoms, 2- Experimental phantoms. While theoretical phantoms are designed with homogeneous and flat layers, voxel phantoms have a structure consisting of a three-dimensional array of voxels. Experimental phantoms, on the other hand, are a type of phantom designed in 4 different types

(liquid, gel, semi-solid and solid) and obtained from materials similar to the dielectric properties of human tissue such as silicon, agar, gelatin saline and sugar. Theoretical phantoms designed in spherical and cylindrical structures are used in EM system and dosimeter studies. Voxel phantoms, on the other hand, are designed to mimic the head, chest and even the whole body based on computed tomography and magnetic resonant images, and are used to evaluate the interaction between the EM spectrum and the human body. Experimental phantoms are phantoms that are generally designed as heads, breasts and limbs and used for microwave imaging studies [41].

### 3.3.1 Breast Phantoms

Human breast tissue consists of two main tissues, adipose and fibroglandular tissues. Adipose tissues determine the structure and shape of the breast, while fibrogulandular tissues include connective tissues, lobular and milk ducts. For early detection of breast cancer, the use of breast phantoms in microwave systems are common in the literature. Solid and semi-solid phantoms are generally fabricated by using ABS, resin, TX-150 and TX-151 materials [42]. Gelatin has an important role in obtaining multilayer phantoms due to its mechanical properties. Usually oil-gelatin or water-gelatin mixtures are used to obtain phantoms. Oil gelatin mixture is more preferred in studies than water mixture. The shelf life of breast phantoms varies due to the materials used in their manufacture, and for this reason, many studies have been carried out to extend their shelf life [43-45]. Due to the fact that breast tissues have different dielectric properties at different frequencies, there are phantom design studies according to different frequency bands. Some of these studies are shown in the table 1 [41].

Table 1: Different Breast phantom design studies

| Frequency | Application | Materials | Tissues | Ref |
|---|---|---|---|---|
| 0.5 GHz–4 GHz | Microwave and US Imaging Modality | Glycerol, Benzalkoniumchloride, Si-C powder, Al2O3-powder, Agar, Deionized water | Breast | [46] |
| 1 GHz – 8 GHz | Microwave Breast Imaging | Polyurethane part-A, Polyurethane part-B, Graphite, Carbon-black, Acetone | Breast tumors | [47] |
| 200 MHz - 6 GHz | Microwave Breast Cancer Detection | P-toluic acid, n-propanol, Deionized water, 200 Bloom Gelatin, Formaldehyde (37% by weight), Oil, Ultra Ivory detergent | Breast tumors (Fat,Gland, Skin) | [48] |
| 3.01 GHz - 11 GHz | Microwave Imaging | Distilled water, Polyethylene powder, Agar, NaCl, Xanthan gum, Sodium, Safflower oil, Propylene glycol, Formalin, Detergent, Surfactant | Breast tumors (Fat, Skin, Muscle) | [9] |
| 50 MHz – 13.51 GHz | Microwave Breast Imaging | Oil, p-toluic Acid, n-propanol, Water, Gelatin, Form, Surfactant | Breast tumors (Fat,Gland, Skin) | [49] |
| 1 GHz – 6 GHz | Heterogeneous Breast Phantom Development for Microwave Imaging | Distilled water, safflower oil, propylene glycol, 200 bloom calf skin, formalin and surfactant | Breast tumors (Fat,Gland, Skin) | [50] |

# Chapter 4

# MICROSTRIP PATCH ANTENNAS

## 4.1 Introduction

Antennas have a majority role in medical applications because they provide communication between sensors and external equipment's. Since microstrip antennas have many advantageous, they are preferred in the field of biomedical applications. In this chapter, brief information about microstrip patch antennas are given and their advantages and disadvantages are mentioned.

## 4.2 Definition of Microstrip Patch Antennas

Microstrip patch antennas comprise of a conductive patch on substrate which is a dielectric material. As illustrated in Figure 5, both the patch and substrate are integrated on a high conductivity metal which is called ground plane. Microstrip patch antennas are fed by transmission lines and both patch and transmission line parts are also high conductivity metals. Microstrip antennas are generally designed as rectangular and circular. While the rectangular antennas preferred because of their simplest analysis, circular antennas are preferred because they have the advantage of radiation [51].

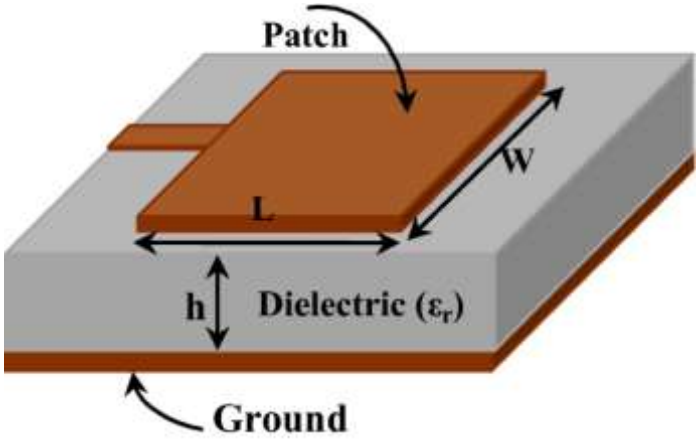


Figure 5: Basic structure of a microstrip patch antenna [52]

Before designing microstrip patch antennas, the resonance frequency and the substrate material to be used must be determined. Substrate material determines the dielectric medium in which the antenna will be designed. The parameters to be calculated are as under [52].

Width of the patch (Wp):

$$W = \frac{C_o}{2f_r}\sqrt{\frac{2}{\varepsilon_r+1}} \tag{4.1}$$

Where, $W$ = Width of the patch, $C_0$= Speed of light and $\varepsilon_r$= value of the dielectric substrate. Radiations traveling from the patch to the ground pass through the air and some through the substrate and causes to occur fringing. The occurred fringing field is a function of effective dielectric constant and causes the antenna length to increase electrically with amount of (ΔL). The value of the effective dielectric constant ($\varepsilon_{reff}$) and the actual increase in length (ΔL) of the patch calculated using the following equation.

$$\varepsilon_{reff} = \frac{\varepsilon_r+1}{2} + \frac{\varepsilon_r-1}{2}\left[1+12\frac{h}{W}\right]^{-1/2}, W/h>1 \tag{4.2}$$

$$\frac{\Delta L}{h} = 0.412\frac{(\varepsilon_{reff}+3)\left(\frac{W}{h}+0.264\right)}{(\varepsilon_{reff}-0.258)\left(\frac{W}{h}+0.8\right)} \tag{4.3}$$

Where h is the height of the substrate.

Length of the patch (Lp):

$$L = \frac{C_o}{2f_r\sqrt{\varepsilon_{reff}}} - 2\,\Delta L \quad (4.4)$$

As mentioned in 4.2, microstrip patch antennas have patch, substrate and ground parts. The length and width of a substrate is equal to that of the ground plane. The length of a ground plane (Lg) and the width of a ground plane (Wg) are calculated using the following equations.

$$L_g = 6h + L \quad (4.5)$$

$$W_g = 6h + W \quad (4.6)$$

## 4.3 Advantageous and Disadvantageous of Microstrip Patch Antennas

Microstrip patch antennas are low profile antennas, which have easy feeding techniques, they can easily fabricate and can be easily used in an array with other microstrip elements. Microstrip antennas have some limitations like having low bandwidth, having lower efficiency than other antennas and even because of the thinner substrates their conductor and dielectric losses can become more severe. Although these situations are considered as disadvantages, they can be improved somehow. For example, their low bandwidth can be improved by some different techniques [53]. In this study square microstrip patch antenna is designed due to the mentioned advantageous of the patch antennas and due to their easy design calculations that mentioned in 4.2.

# Chapter 5

# INVESTIGATION OF BREAST CANCER IN BREAST PHANTOM USING WEARABLE PATCH ANTENNA

## 5.1 Introduction

In this study, a wearable microstrip patch antenna that can operate in the ISM band (2.4 GHz) was designed to detect the breast cancer using the CST Microwave Studio. Since bio-incompatibility may occur in the use of implantable antennas, it is preferred to design a wearable antenna due to its applicability and portability. On the other hand, two breast phantoms for fat, skin, gland and tumor have been designed from a combination of everyday chemicals and this realistic breast phantom has been used in microwave detection of breast cancer. Thus, tumor and tumor-free breast tissues were determined according to the differences between the reflection coefficients. As it mentioned in Chapter 3, according to WHO the early detection of the breast tumor is important to reduce the number of deaths from breast cancer. Accordingly, in this study, an antenna that can detect both early stages and second stages of breast tumor was designed by using tumor models with 0.5,2 and 5 cm sizes. This antenna, was made of copper annealed conductor implemented on FR4 substrate with relative dielectric constant 4.3, thickness 1.6 mm and is operating at 2.4 GHz. To test the antenna, two tissue mimic breast phantoms, which are normal and infected, was designed in a laboratory and antenna's return loss was measured on the phantoms.

## 5.2 Antenna Design

28.8 x 28.8 $mm^2$ patch antenna which implemented on FR4 structure with 1.6 mm thickness and relative permittivity 4.3 has designed and fed with a 50 ohm microstrip line with 3.05 mm width by using CST Microwave Studio. The dimensions of the whole antenna are given in the Table 2 and Figure 6 illustrates the designed and fabricated antenna. The antenna was designed to operate at 2.4 GHz in free space and then optimized for the normal breast phantom by following certain steps and strategies. The optimization details are given in detail in the Appendix section.

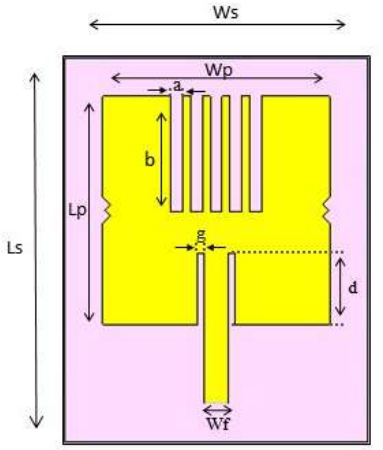


a

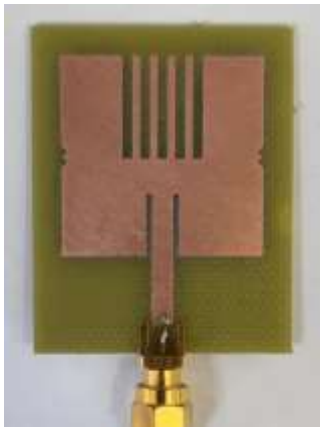

b

Figure 6: (a) Designed antenna, (b) Fabricated antenna

Table 2 : Antenna dimensions

| Parameters | Dimensions (mm) |
|---|---|
| Patch Width (Wp) | 28.8 |
| Patch Length (Lp) | 28.8 |
| Substrate/Ground Width (Ws) | 38.4 |
| Substrate/Ground Length (Ls) | 38.4 |
| Thickness of Patch / Ground (t) | 0.035 |
| Thickness of Substrate (h) | 1.6 |
| Feedline Width (Wf) | 3.05 |
| Inset Length (d) | 9 |
| Gap (g) | 0.85 |
| A | 1.45 |
| B | 15 |
| C | 1 |

Figure 7 shows the return loss of the antenna in free space and Figure 8 illustrates the electric and magnetic far field radiation patterns of the antenna in free space.

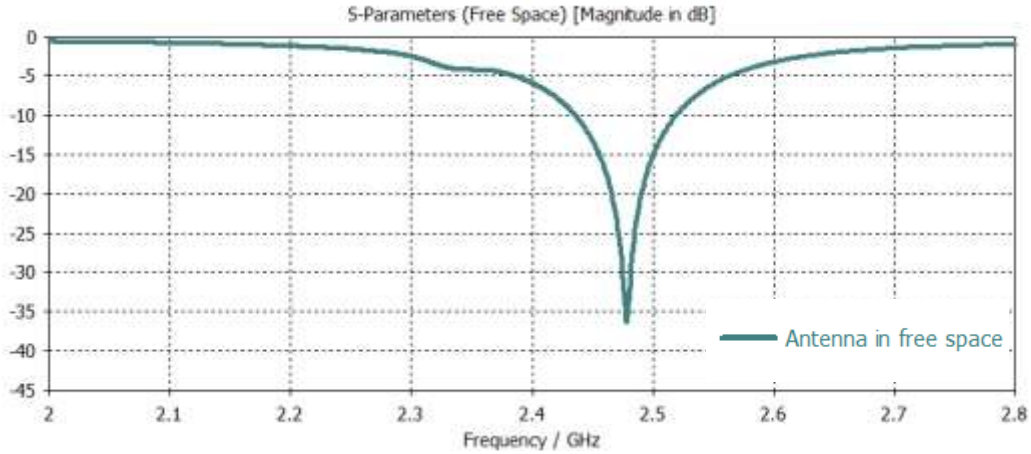


Figure 7: Simulated return loss of the antenna in free space

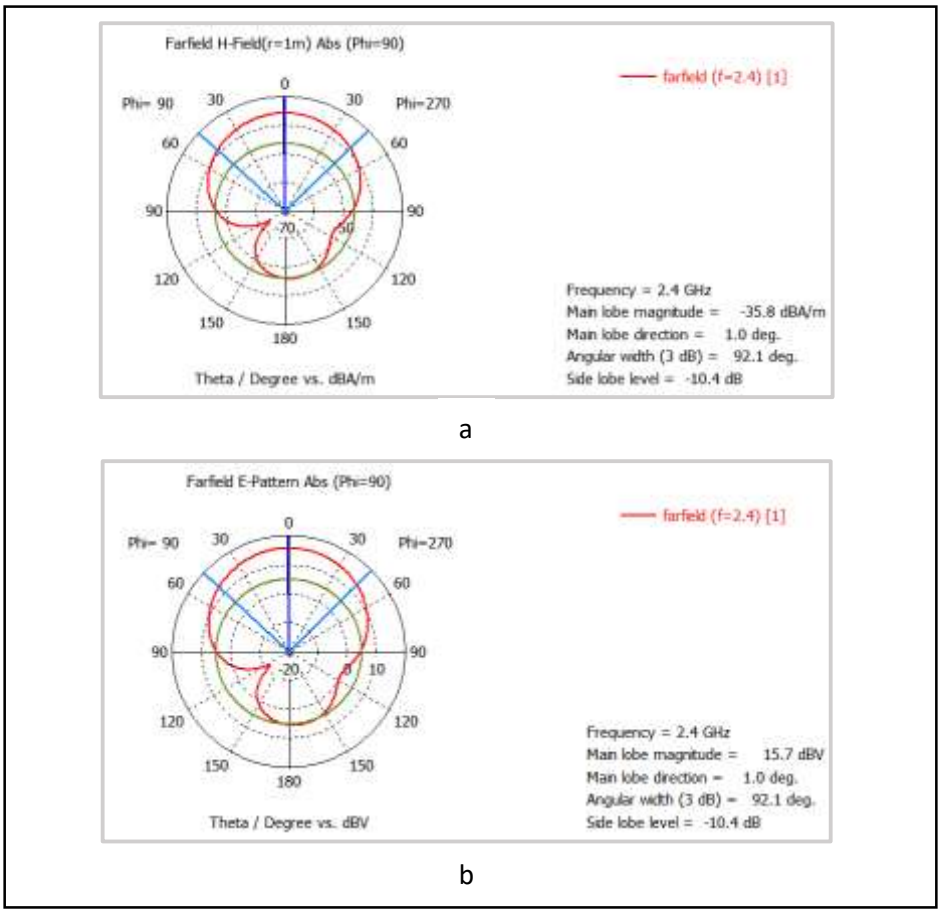


Figure 8: H and E plane far field radiation pattern. (a) H field, (b) E field.

## 5.3 Breast Phantom Design Using CST Microwave Studio

In order to observe the difference between normal and tumor breast cells and to optimize the designed antenna, a breast phantom consisting of 3 layers, which are skin, fat and glandular, was created as shown in the Figure 9.

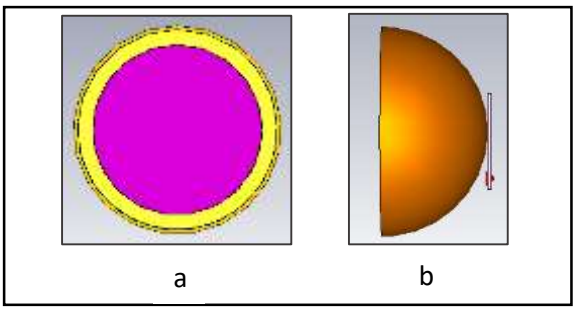


Figure 9: Designed breast phantom model in CST Microwave Studio.
(a) Back view, (b) Side view

The breast phantom model was designed as a semi-spherical model with a diameter of 110 mm and was created according to the permeability and conductivity values of real breast tissues at 2.4 GHz microwave frequency [50]. The dimensions and electric properties of the breast phantom is given in the table 3 and Fig 10, illustrates the return loss of the antenna (-43 dB) when it is on the normal breast phantom.

Table 3 : Dimensions and the dielectric properties of the breast phantom

| Material | Permittivity (ε) | Conductivity S/m (σ) | Diameter (mm) |
|---|---|---|---|
| Skin | 38 | 1 | 110 |
| Fat | 5 | 0.1 | 106 |
| Glandular | 45 | 1.8 | 90 |
| Tumor | 55 | 2.5 | 5, 20, 50 |

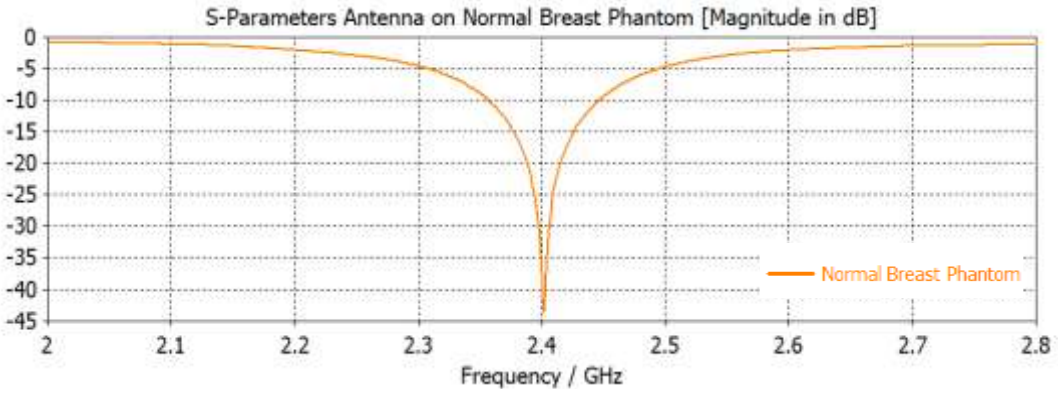


Figure 10: Simulated return loss values of antenna on the breast phantom

After simulation of the antenna on the normal breast phantom, 0.5, 2 and 5 cm tumors were designed in the breast phantom to study stage I and stage II cancer stages. The tumors were designed with a permittivity of 55 and conductivity of 2.5 S/m [54] and placed horizontally at a distance of 10 mm from the nipple of the breast phantom as shown in Figure 11.

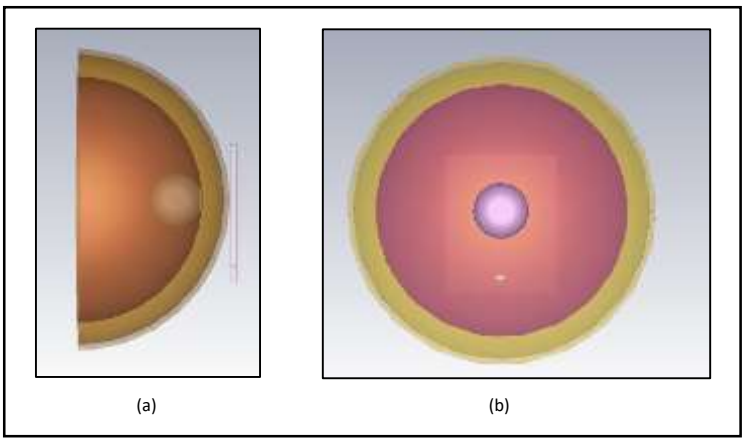


Figure 11: Location of the infected phantom.
(a) Side view, (b) Back view

Figure 12 shows the return loss simulations of the antenna on infected breast phantom with 0.5, 2 and 5 cm tumors. Since the permittivity and conductivity values of the tumor are higher than the breast tissues, the presence of the tumor is expected to cause changes in return loss. Figure 12 shows the return loss curves for different tumor sizes. It was observed from the results that as the tumor size increased, the return loss value increased from 33 dB to 31 dB and 29 dB for 0.5, 2 and 5 cm tumor presence respectively. Figure 13 illustrates the difference in simulated antenna return loss values between the normal and infected breast phantom.

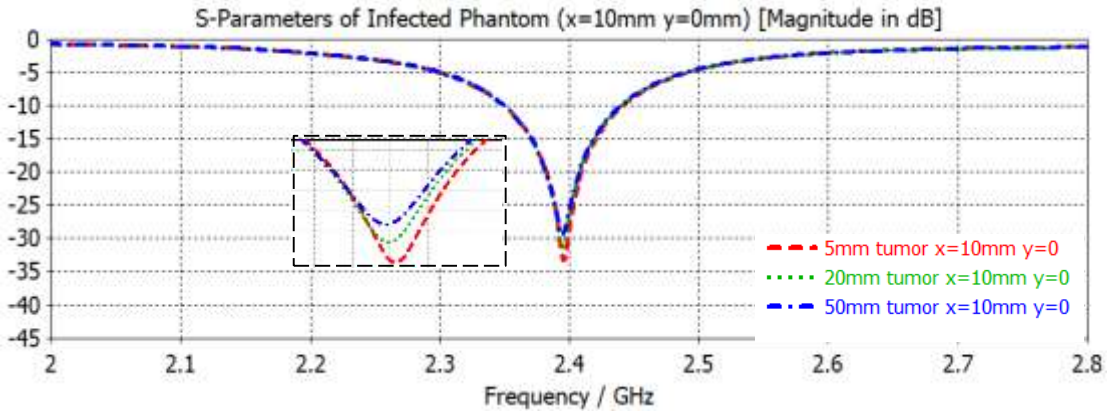


Figure 12: Simulated return loss values of the antenna on infected breast phantom

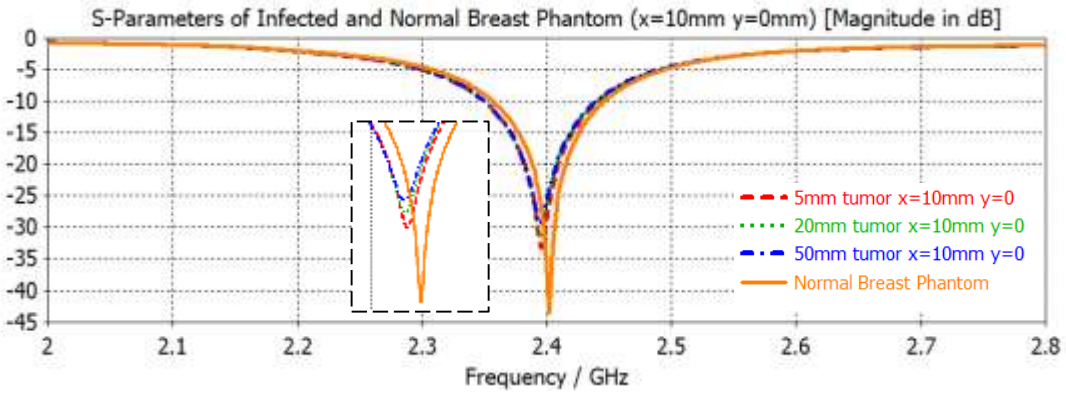


Figure 13: Simulated return loss values of the antenna on healthy and infected breast phantom

Although expected results were seen when tumor tissue was placed horizontally, the tumor was placed 10 mm up and 10 mm down on the vertical axis and 10 mm inward on the horizontal axis to test the feasibility of tumor detection in other positioning of the tumor and, simulations were taken. Figure 14 illustrates the position of the tumor placed vertically. According to Figure 15 which illustrates the return loss values obtained by positioning the tumor 10 mm up and 10 mm down, it was observed that the return loss value increased as the tumor size increased. So even if the tumor position changed, the change in the return loss values of the antenna at different tumor diameter proved the accuracy of the designed antenna. Thus, we can conclude that the designed antenna can detect tumor regardless of tumor location.

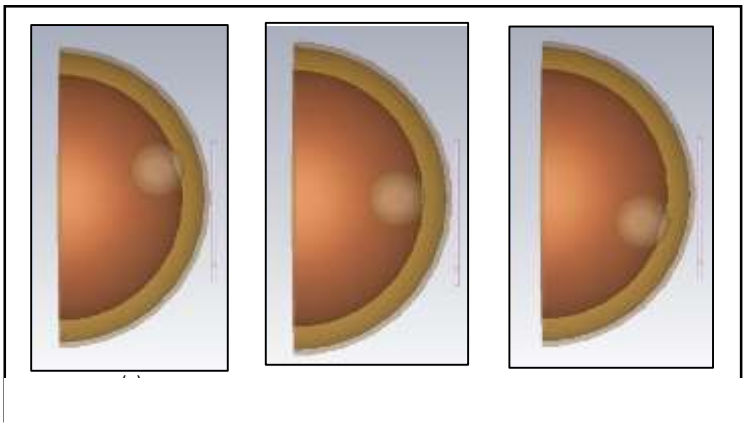

Figure 14: Different positions of the tumor
(a) x=10 y=10 , (b) x=10 y=0, (c) x=10 y= -10

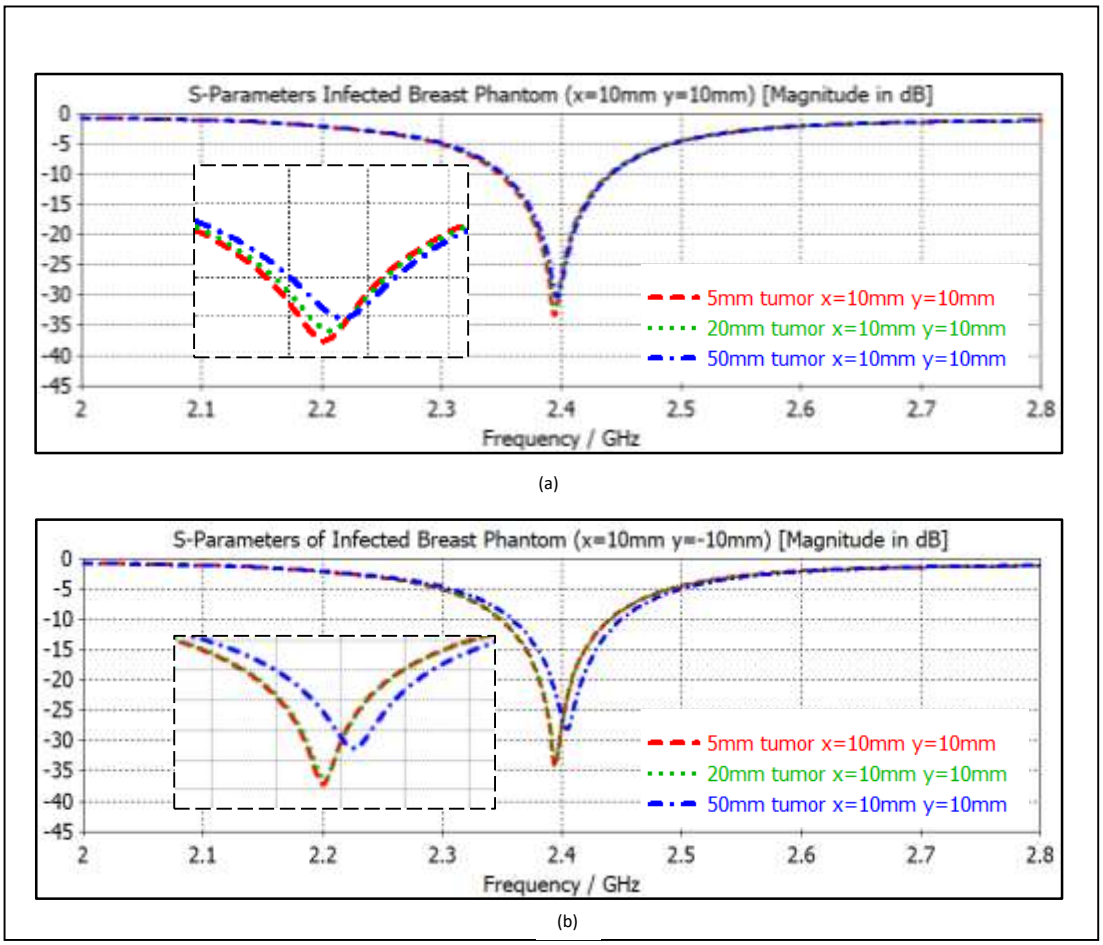


Figure 15: Simulated return loss values obtained by positioning the tumor 10 mm up and 10 mm down. (a) x=10 y=10, (b) x=10 y= -10

## 5.4 Tissue Mimic Breast Phantom Development

As detailed in Chapter 3.3, tissue mimic phantoms are used for the development and testing of microwave antennas. These structures, which are designed to imitate human tissue, make the experiments that need to be done on humans easier and easily take measurements for optimizing, developing and evaluating microwave imaging systems without resorting to procedures such as ethical committees.

A heterogeneous breast phantom with 3 layers (skin, fat, glandular) that can have human breast tissue characteristics at 2.4 GHz was fabricated in this thesis. In order to achieve successful results in microwave antenna studies, it is important that the

phantom resembles human tissues in terms of its physical and dielectric properties. Based on this principle, a model was studied both in dielectrically close to the breast tissues and physically close to the real breast. While obtaining the phantom, the values in the study of Camein et al., [50] were taken as reference. Camein et al., basically tried to obtain the permittivity and conductivity values of the human breast tissues based on 4 materials (propylene glycol, distilled water, oil and gelatin). Before combining the materials, they measured the dielectric properties of each material and performed a regressing analysis to determine the amount of each material. As a result, they approached the expected permittivity value by using water with high permittivity values, while they approached the expected conductivity value by taking advantage of the low conductivity of propylene glycol and oil. They used gelatin to obtain a solid gel structure. At the end of the study, they obtained a heterogeneous 4-layer breast phantom consisting of skin, fat, glandular and transitional layer, which can mimic the breast between 1 and 5 GHz microwave frequencies.

In this study, firstly one healthy breast phantom consisting of 3 layers was obtained and then one infected phantom consisting of 3 layers with 2 cm cylindrical phantom, which could mimic the tumor, was obtained. During the fabrication of the heterogeneous healthy phantom, distilled water, safflower oil, propylene glycol, 200 bloom calf-skin gelatin, formalin and surfactant were used and for the infected phantom fabrication distilled water, ethanol, sodium chloride and agarose were used. In addition, orange food coloring was used for the skin layer and purple food coloring was used for the glandular layer in order to distinguish the layers from each other. The materials and mixing ratios for the layers of the phantom (skin, fat, glandular and tumor) are listed in Table 3. To make the shape of the breast phantoms physically

resemble the breast, as shown in Figure 16, three molds designed from foil paper in the form of a semi-cylindrical shape. Since the breast phantom consists of three layers, the liquids for each layer were prepared separately and the phantom was produced in three stages. As shown in Figure 17, first the glandular part was prepared and poured into a 4.5 cm mold, then kept in the freezer for half an hour to solidify. In the second stage, the liquid for the fat was prepared and poured into a 5.3 cm mold and the solid glandular structure was placed on it and kept in the refrigerator for the same time. In the third stage, the liquid for the skin was poured into a 5.5 cm mold. Glandular and fat structure was placed on it and kept in the refrigerator for one night. As the healthy phantom was ready after one night, measurements were taken using the NanoVNA-F V2 Vector Network Analyzer. Molds with radii of 5.5 cm, 5.3 cm and 4.5 cm were used. Afterwards, for the infected phantom, tumor tissue was obtained by referring to the study of Ortega et al., [54] glandular layer was obtained by placing the obtained tumor phantom in a 4.5 cm mold. Afterwards, the steps when a healthy phantom was obtained were applied to fabricate the infected phantom. The procedure of the phantom fabrication for each layer is represented in detailed by a flow chart in the Figure 17. Both of the healthy and infected phantoms displayed in Figure 18.

Table 4: List of materials and quantities used for each layer

| Material | Quantity | | | |
|---|---|---|---|---|
| | Skin | Fat | Glandular | Tumor |
| Distilled water | 80 mL | 40 mL | 80 mL | 100 mL |
| Safflower oil | 15.20 mL | 42.35 mL | 22.80 mL | - |
| Propylene glycol | 6.75 | 1.93 mL | 6.75 mL | - |
| 200 Bloom calf-skin gelatin | 5.88 g | 7.00 g | 5.00 g | - |
| Formalin (37% formaldehyde solution) | 0.275 mL | 0.275 mL | 0.275 mL | - |
| Surfactant | 0.283 mL | 0.283 mL | 0.283 mL | - |
| Ethanol | - | - | - | 60 mL |
| NaCl | - | - | - | 1.00 g |
| Agarose | - | - | - | 1.5 g |

(a) (b) (c)

Figure 16: Molds that are used in breast phantom design.
(a) 55 mm semi-spherical mold for skin, (b) 53 mm semi- spherical mold for fat, (c) 45 mm semi- spherical mold for glandular

**Healthy and Infected Breast Phantom Fabrication**

1. Divide the materials into containers according to the specified quantities for each layer

2.Start with Glandular layer

Distilled water

Propylene glycol

3. Use double boiler to heat the compounds. Mix until temperature reaches 50℃

Gelatin

4. Mix until it dissolve

Formalin

Surfactant

Oil

5. Stop heating and put the mixture in a bowl of ice. Mix until the temperature reaches 30 ℃

6. Pour the mixture to the 4.5 cm mold and kept it in the fridge for half an hour

7. To prepare the fat layer, return to step3 and prepare the mixture

8. Pour the mixture to the 5.3 cm mold and place the solidified glandular layer on it. and kept it in the fridge for half an hour

9. To prepare the skin layer, return to step 3 and prepare the mixture

10. Pour the mixture to the 5.5 cm mold and place the solidified glandular and fat layer on it. Kept it in the fridge overnight

**Healthy and Infected Breast Phantom Fabrication Continue**

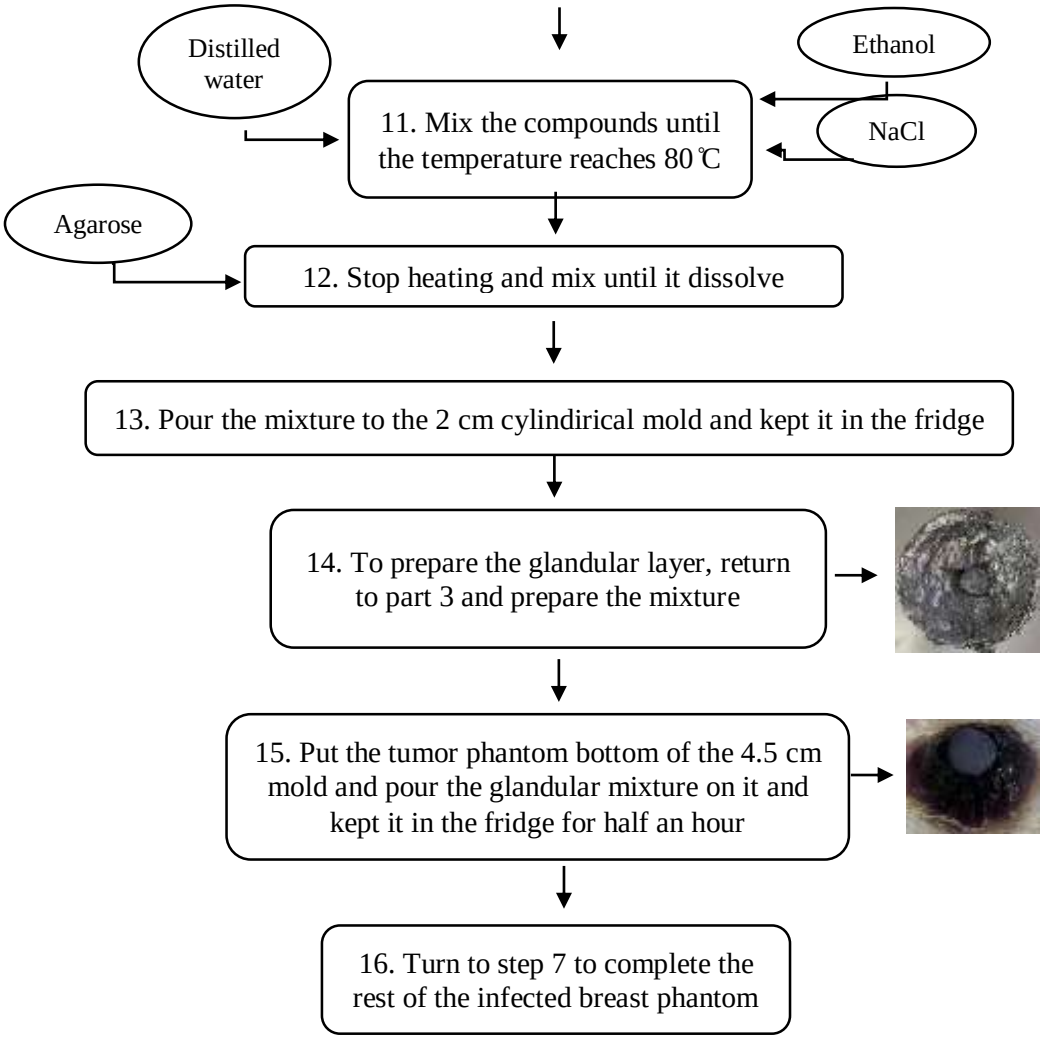


Figure 17: Tissue mimic breast phantom preperation steps

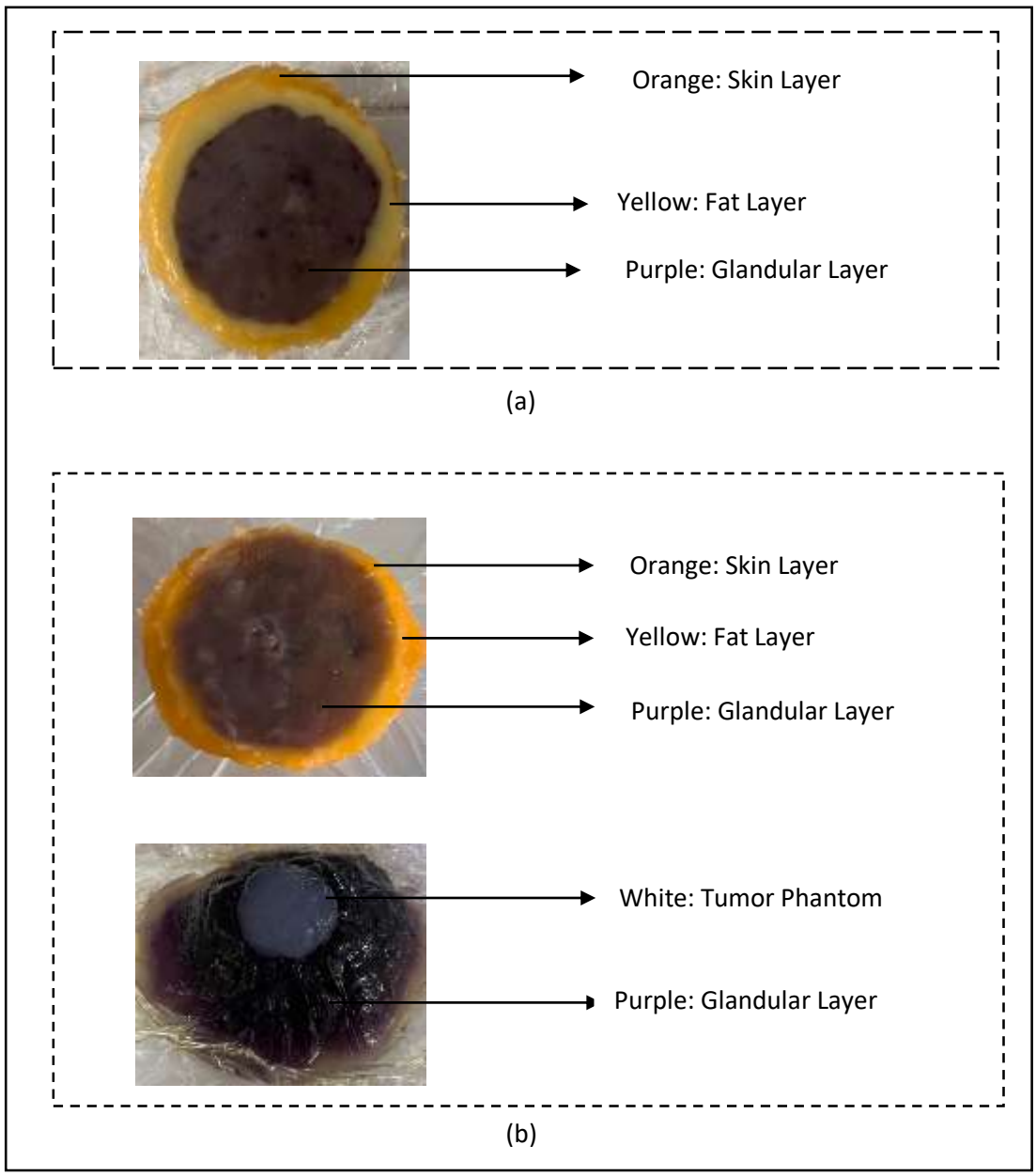


Figure 18: Fabricated tissue mimic healthy and infected breast phantom.
(a) Healthy breast phantom, (b) Infected breast phantom

## 5.5 Simulation and Measured Results

As explained in detailed in 5.3, in order to observe the effect of tumor tissues on return loss different tumor sizes were adjusted and simulations were taken. In addition, in order to test the validation of the designed antenna, realistic breast phantoms were designed and measurements were taken on fabricated phantoms. All simulations were done by using CST Microwave Studio and all measurements were done by using the

NanoVNA-F V2 Vector Network Analyzer. The position of the antenna while taking the measurement and simulation of the return loss values of tumor and normal breast phantoms is as shown in Figure 19.

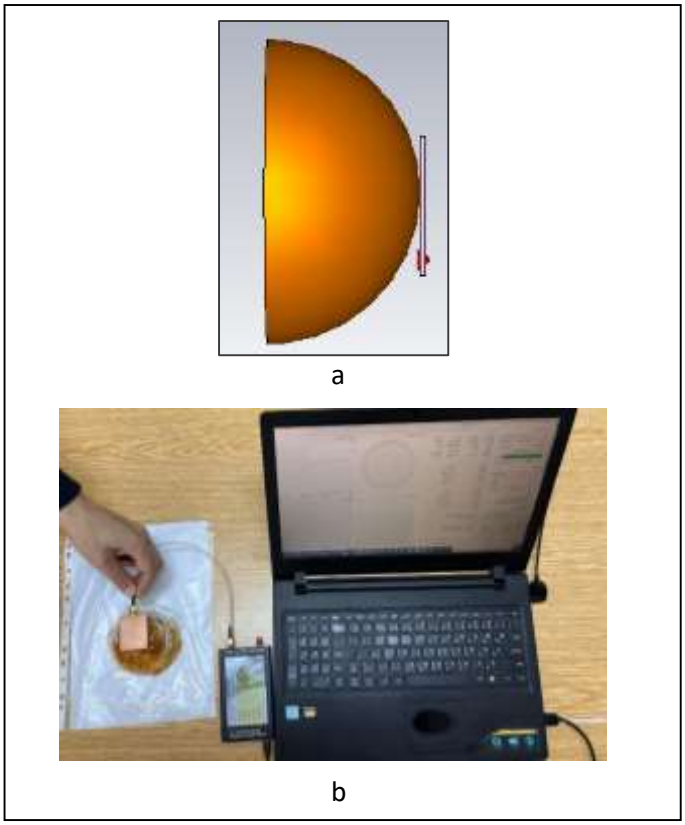


Figure 19: Figure 19: Antenna positions.
(a) Antenna position during simulations
(b) Antenna position during measurements

The measured and simulated return loss of the designed antenna in free space is shown in Figure 20. In simulations antenna resonates at 2.478 GHz with -36.33 dB and in measurements it has been observed that it has matched resonance frequency but has a return loss of -26 dB.

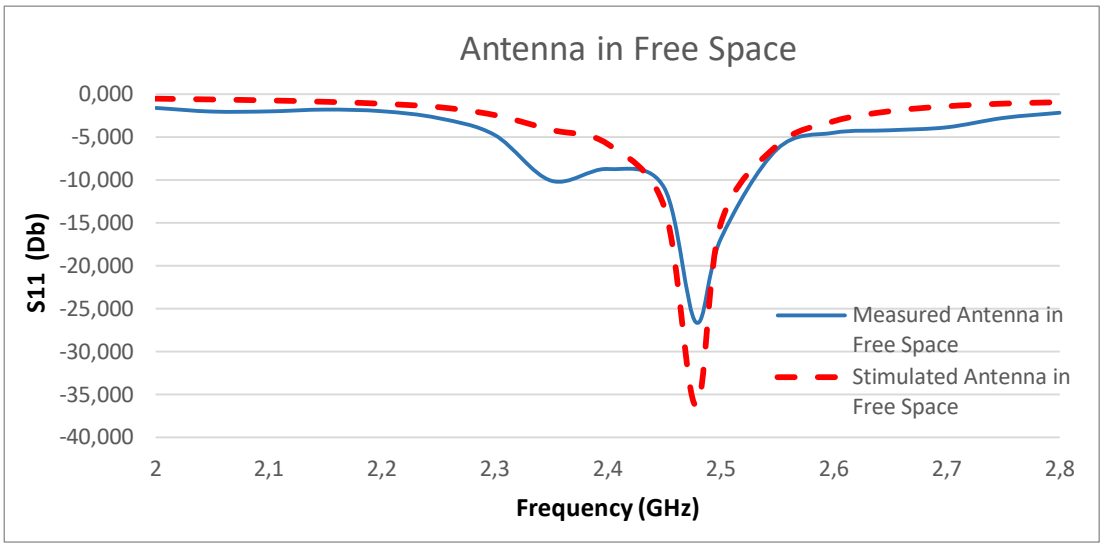


Figure 20: Measured and simulated return loss values for the antenna in free space

Figure 21 illustrates the return loss simulated and measured results of the antenna placed on the healthy breast phantom. In both cases the antenna resonates at 2.4 GHz with different return loss values (-43 dB observed from simulations and -28 dB observed from measurements). Although the return loss curves have similar behavior, differences can be observed between simulation and measurement of return loss values. These differences are due to the effects surrounding the antenna, such as the laboratory environment, designed phantom and accuracy of the antenna.

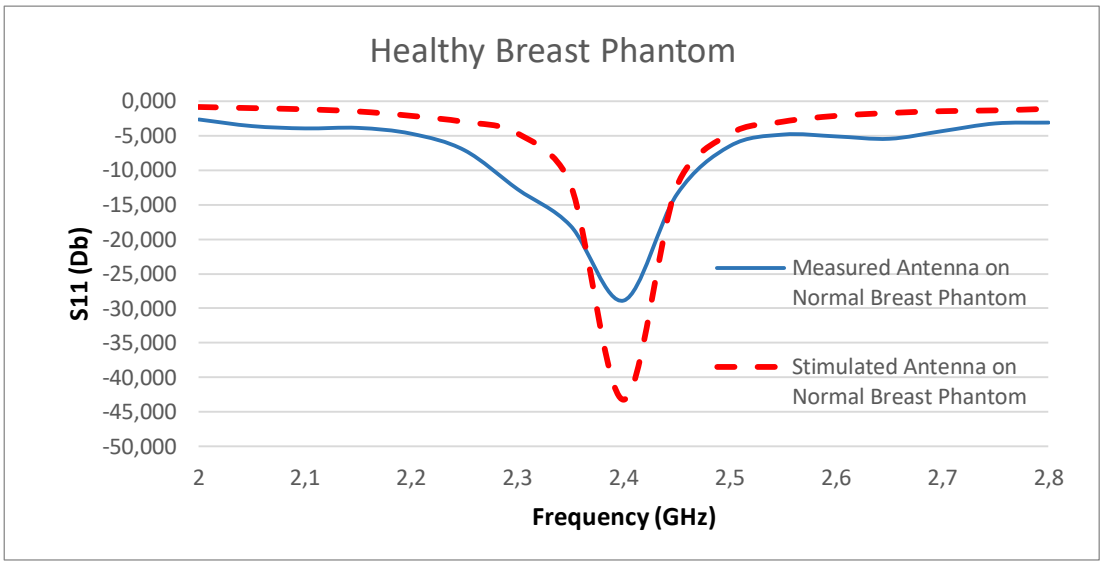


Figure 21: Measured and simulated return loss values when the antenna is placed on the healthy breast phantom

Figure 22 depicts the simulation of antenna on infected and normal breast phantom. To define stage I, and stage II cancers the tumors radii was adjusted to 0.5 cm 2 cm and 5 cm. In the simulations, it was observed that the return loss values increased with the presence of the tumor and the enlargement of its radii. While the healthy phantom had a minimum return loss value of -38 dB, 0.5 cm, 2 cm and 5 cm tumors were observed to be approximately -33 dB, -31 dB and -28 dB, respectively.

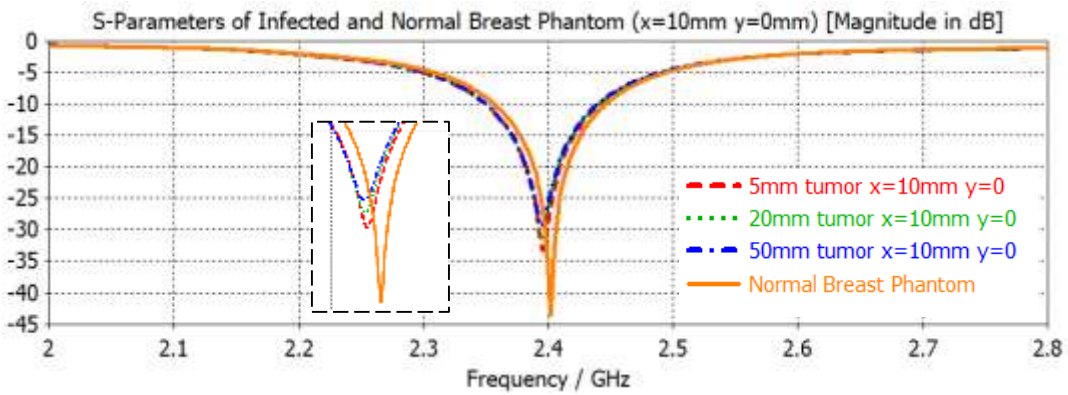


Figure 22: : Simulated return loss values when the antenna is placed on healthy and infected breast phantom

In order to make tumor detection according to return loss values, it is expected that there will be an increase in return loss values in tumor formation. Although this situation was proven in simulations, measurements were carried out on fabricated realistic phantoms with and without tumors to test the accuracy of the antenna. In order to observe the change in return loss value in the presence of a tumor, measurement was taken on the infected phantom with 2 cm tumor. In the measurements taken on the infected phantom, it was observed that the minimum return loss value was -16dB at 2.4 GHz. Thus, as shown in the Figure 23, while the return loss value was -26 dB in the measurements on the normal breast phantom, it was observed that the return loss value increased to -16 dB in the measurements on infected breast phantom tissue. Thus expected results have been achieved and it is concluded that the change in the return loss value in the presence of tumor is in the same direction in the measurements and simulations.

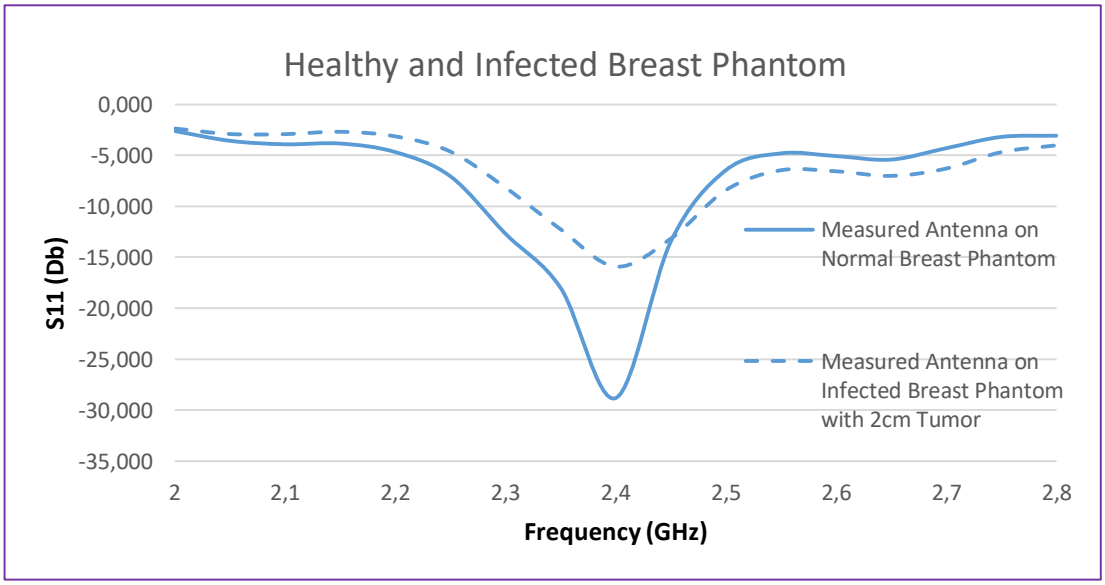


Figure 23: Measured return loss values when the antenna is placed on healthy and infected breast phantoms

Figure 24 illustrates the difference between simulations and measurements of normal and 2 cm tumorous phantoms return loss values. The measurement shows a good matching with simulation. Difference between the simulations and measurements can be related to surrounding environments.

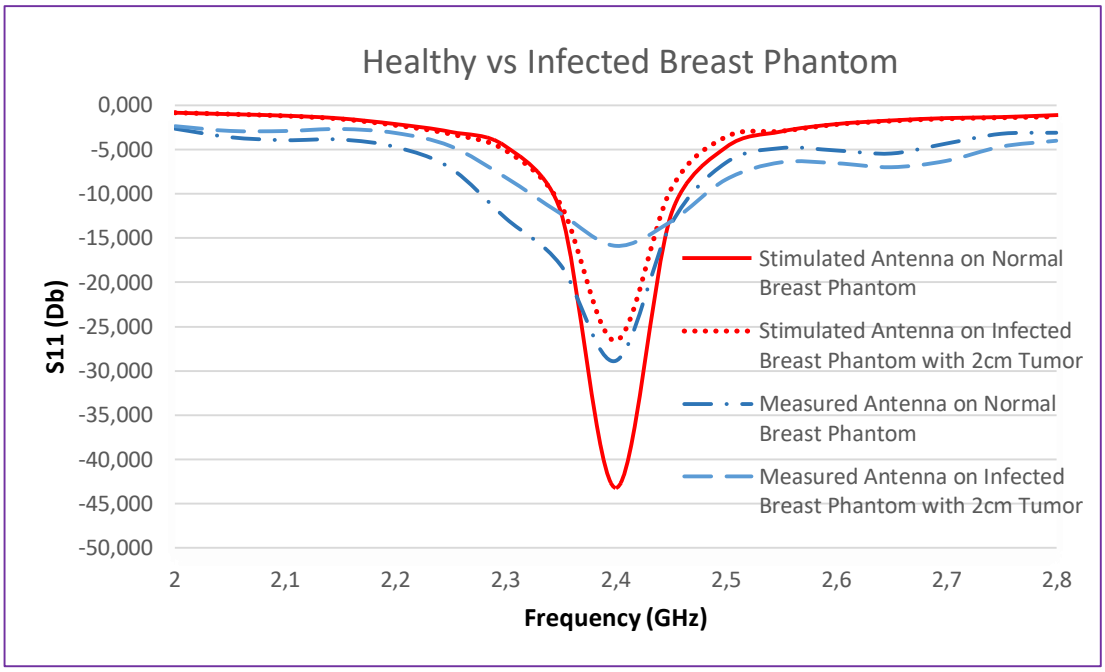


Figure 24: Simulated and measured return loss values when the antenna is placed on healthy and infected breast phantom

## 5.6 Specific Absorption Rate (SAR)

Specific Absorption Rate is a measure of the body's absorption rate of electromagnetic energy per unit mass in watts (W/kg). Since this work is related to the human body, SAR values of human tissues should be taken into consideration. The absorption rate is affected by transmitted power and antenna positions. SAR is related to the conductivity, tissues mass density and RMS values of the electric field components [55]. The European pick limit of the SAR is accepted as 2 W/kg over average of 10 g of tissues [56].

Since the mass density of the tissues should be taken into account when calculating the SAR value, in this study the mass density values of the breast phantom layers is adjusted and then the SAR value is calculated by using CST Microwave Studio. Mass density of the skin adjusted as 972 kg/m$^3$, mass density of the fat adjusted as 890 kg/m$^3$ and mass density of the glandular tissue adjusted as 900 kg/m$^3$ [57]. The maximum SAR value is calculated as 1.09 W/kg over 10 g and depicted in Figure 25.

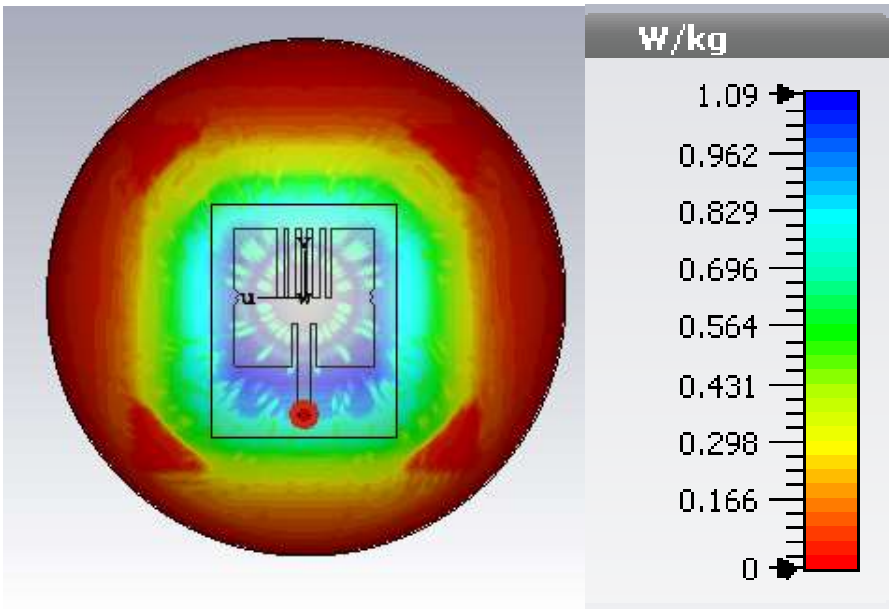


Figure 25: Simulated SAR for the antenna implanted on the healthy breast phantom

# Chapter 6

# CONCLUSION

This thesis outlines the breast cancer detection using dielectric properties of the human breast at Industrial, Scientific, and Medical (ISM)frequency band (2.4 GHz to 2.4835 GHz). The permittivity, conductivity and thickness of skin, fat and glandular layers are specified for healthy and infected breast tissues and a realistic breast phantom was designed according to these parameters. Depending on these electrical properties, the scattering properties of the electromagnetic wave impinging to the human body show differences in healthy and infected tissues.

28.8 x 28.8 $mm^2$ patch antenna which implemented on FR4 structure with 1.6 mm thickness and relative permittivity 4.3 has been designed and fabricated. Antenna was fed with a 50 Ω micro strip line with 3.05 mm width for good matching with the source.

Main idea of this study is to take and compare return loss simulations and measurements on healthy and infected phantom for the detection purpose of the cancerous tissues. Accordingly, the antenna was placed on the breast phantom and different return loss responses were obtained from healthy and infected tissues.

Breast phantom model consisting of 3 layers as skin, fat and glandular were introduced and fabricated in this thesis with relative dielectric constant and electrical conductivities of 38, 1 S/m, 5, 0.1 S/m, 45 and 1.8 S/m respectively. Also a tumorous

breast phantom with permittivity of 55 and conductivity of 2.5 S/m was handled as an infected breast phantom. The return loss was simulated on the healthy and infected breast phantom model and measurements were taken on the realistic fabricated healthy and infected phantom and the return loss values of the antenna was used to detect the tumorous tissues.

During the simulations the tumor radius values of 0.5 mm, 20 mm and 50 mm were considered. First, the tumor was placed at a depth of 1 cm for each value and then the horizontally distance was kept constant and the tumor distance was change vertically to 1 cm up and 1 cm down for each value (x=10 y=0, x=10 y=10, x=10 y=-10). It was concluded that increasing the tumor radius increases the return loss value. On the other hand, to test the simulations, an infected realistic breast phantom with 20 mm tumor was fabricated. The measurements were taken on both fabricated healthy and infected phantoms and it was also concluded that the presence of the tumor increases the return loss value. It can be said that, the simulations carried out by CST Microwave Studio are in a good agreement with the measured results of the realistic tissue mimic breast phantoms.

It is concluded form the simulations and measurements of the fabricated tissue mimic phantom that presence of the tumor changes the values of the return loss. Moreover, increasing the radius of tumors cells increases the return loss values. On the hand the adopted analysis can sense the case of early stage I and stage II of the cancer in the body. Furthermore, acceptable results were simulated for the SAR.

# REFERENCES

[1] Arnold, M., Morgan, E., Rumgay, H., Mafra, A., Singh, D., Laversanne, M., ... & Soerjomataram, I. (2022). Current and future burden of breast cancer: Global statistics for 2020 and 2040. The Breast, 66, 15-23.

[2] Ginsburg, O., Yip, C. H., Brooks, A., Cabanes, A., Caleffi, M., Dunstan Yataco, J. A., ... & Anderson, B. O. (2020). Breast cancer early detection: A phased approach to implementation. *Cancer*, *126*, 2379-2393.

[3] Paci, E. (2002). Nass SJ, Henderson IC, Lashof JC (eds): Mammography and Beyond: Developing Technologies for Early Detection of Breast Cancer. Washington, DC: National Academy Press, 2001. 316 pp. *Breast Cancer Research*, *4*(3), 1-3.

[4] Jahan, I., & Kabir, A. (2021, December). Microstrip Patch Antenna for Breast Cancer Detection. In 2021 5th International Conference on Electrical Information and Communication Technology (EICT) (pp. 1-6). IEEE.

[5] Dharani, K. R., Sampath, P., Soukath, A. K., Pavithra, D., & Renuga, D. M. (2014, February). Design and simulation of microstrip phased array antenna for biomedical applications. In *2014 International Conference on Electronics and Communication Systems (ICECS)* (pp. 1-6). IEEE.

[6] Ali, N., Sree, M. A., Uyguroglu, R., & Allam, A. M. M. A. (2020). Stage II cancer detection using printed antenna implemented on hemispherical model for human breast. *Journal of Instrumentation*, *15*(09), P09016.

[7] Mobashsher, A. T., & Abbosh, A. M. (2015). Artificial human phantoms: Human proxy in testing microwave apparatuses that have electromagnetic interaction with the human body. *IEEE Microwave Magazine*, *16*(6), 42-62.

[8] Kumar, H. V., & Nagaveni, T. S. (2020). Design of microstrip patch antenna to detect breast cancer. *ICTACT Journal On Microelectronics*, *6*(01).

[9] Islam, M. T., Samsuzzaman, M., Islam, M. T., Kibria, S., & Singh, M. J. (2018). A homogeneous breast phantom measurement system with an improved modified microwave imaging antenna sensor. sensors, 18(9), 2962.

[10] Gupta, A., Kansal, A., & Chawla, P. (2021). A survey and classification on applications of antenna in health care domain: data transmission, detection and treatment. Sādhanā, 46(2), 1-17.

[11] Basar, M. R., Malek, F., Juni, K. M., Idris, M. S., & Saleh, M. I. M. (2012). Ingestible wireless capsule technology: A review of development and future indication. *International Journal of Antennas and Propagation*, *2012*.

[12] Lee, S. H., Lee, J., Yoon, Y. J., Park, S., Cheon, C., Kim, K., & Nam, S. (2011). A wideband spiral antenna for ingestible capsule endoscope systems:

Experimental results in a human phantom and a pig. IEEE Transactions on Biomedical Engineering, 58(6), 1734-1741

[13] El Hatmi, F., Grzeskowiak, M., Protat, S., & Picon, O. (2013). Link budget of magnetic antennas for ingestible capsule at 40 MHz. Progress In Electromagnetics Research, 134, 111-131.

[14] Liu, C., Guo, Y. X., & Xiao, S. (2014). Circularly polarized helical antenna for ISM-band ingestible capsule endoscope systems. IEEE Transactions on Antennas and Propagation, 62(12), 6027-6039.

[15] Hong, Y., Tak, J., & Choi, J. (2016). An all-textile SIW cavity-backed circular ring-slot antenna for WBAN applications. IEEE Antennas and Wireless Propagation Letters, 15, 1995-1999.

[16] Agneessens, S. (2017). Coupled eighth-mode substrate integrated waveguide antenna: Small and wideband with high-body antenna isolation. IEEE Access, 6, 1595-1602.

[17] Ashyap, A. Y., Zainal Abidin, Z., Dahlan, S. H., Majid, H. A., & Saleh, G. (2019). Metamaterial inspired fabric antenna for wearable applications. International Journal of RF and Microwave Computer-Aided Engineering, 29(3), e21640.

[18] Al-Sehemi, A., Al-Ghamdi, A., Dishovsky, N., Atanasov, N., & Atanasova, G. (2017). On-body investigation of a compact planar antenna on multilayer polymer

composite for body-centric wireless communications. AEU-International Journal of Electronics and Communications, 82, 20-29.

[19] Malik, N. A., Sant, P., Ajmal, T., & Ur-Rehman, M. (2020). Implantable antennas for bio-medical applications. *IEEE Journal of Electromagnetics, RF and Microwaves in Medicine and Biology*, *5*(1), 84-96.

[20] Karacolak, T., Cooper, R., & Topsakal, E. (2009). Electrical properties of rat skin and design of implantable antennas for medical wireless telemetry. IEEE Transactions on Antennas and Propagation, 57(9), 2806-2812.

[21] Kaur, G., Kaur, A., Toor, G. K., Dhaliwal, B. S., & Pattnaik, S. S. (2015). Antennas for biomedical applications. Biomedical Engineering Letters, 5(3), 203-212.

[22] Imran, A. I., & Elwi, T. A. (2017). A cylindrical wideband slotted patch antenna loaded with frequency selective surface for MRI applications. Engineering Science and Technology, an International Journal, 20(3), 990-996.

[23] Davis S K, Veen V, Hagness B D and Kelcz F. (2008). Breast tumour characterization based on ultrawideband microwave backscatter. IEEE Trans. Biomed. Eng. 55: 237–246.

[24] Ahmed, S. S., Schiessl, A., Gumbmann, F., Tiebout, M., Methfessel, S., & Schmidt, L. P. (2012). Advanced microwave imaging. IEEE microwave magazine, 13(6), 26-43.

[25] Jamlos, M. A., Jamlos, M. F., & Ismail, A. H. (2015, April). High performance novel UWB array antenna for brain tumor detection via scattering parameters in microwave imaging simulation system. In *2015 9th European Conference on Antennas and Propagation (EuCAP)* (pp. 1-5). IEEE.

[26] Kaur, G., & Kaur, A. (2021). Monostatic radar-based microwave imaging of breast tumor detection using a compact cubical dielectric resonator antenna. Microwave and Optical Technology Letters, 63(1), 196-204.

[27] Ali, N., Uyguroglu, R., & Allam, A. M. M. A. (2018). Cancer detection in breast using biological and electromagnetic properties of breast tissues on antenna performance. In *2018 18th Mediterranean Microwave Symposium (MMS)* (pp. 325-329). IEEE.

[28] Ryan, T. P., & Brace, C. L. (2017). Interstitial microwave treatment for cancer: historical basis and current techniques in antenna design and performance. International Journal of Hyperthermia, 33(1), 3-14.

[29] Qian, G. J., Wang, N., Shen, Q., Sheng, Y. H., Zhao, J. Q., Kuang, M., ... & Wu, M. C. (2012). Efficacy of microwave versus radiofrequency ablation for treatment of small hepatocellular carcinoma: experimental and clinical studies. European radiology, 22(9), 1983-1990.

[30] Zimmerman, J. W., Jimenez, H., Pennison, M. J., Brezovich, I., Morgan, D., Mudry, A., ... & Pasche, B. (2013). Targeted treatment of cancer with

radiofrequency electromagnetic fields amplitude-modulated at tumor-specific frequencies. Chinese journal of cancer, 32(11), 573.

[31] Glassberg, M. B., Ghosh, S., Clymer, J. W., Qadeer, R. A., Ferko, N. C., Sadeghirad, B., ... & Amaral, J. F. (2019). Microwave ablation compared with radiofrequency ablation for treatment of hepatocellular carcinoma and liver metastases: a systematic review and meta-analysis. OncoTargets and therapy, 12, 6407.

[32] Wright, A. S., Sampson, L. A., Warner, T. F., Mahvi, D. M., & Lee, Jr, F. T. (2005). Radiofrequency versus microwave ablation in a hepatic porcine model. Radiology, 236(1), 132-139.

[33] Schipf, S., Knüppel, S., Hardt, J., & Stang, A. (2011). Directed Acyclic Graphs (DAGs)–Die Anwendung kausaler Graphen in der Epidemiologie. Das Gesundheitswesen, 73(12), 888-892.

[34] Park, C. B., & Ng, C. Clinical description of a bronchoscopic approach to ablate lung nodules using the Emprint™ Ablation Catheter Kit with Thermosphere™ Technology.

[35] Savci, H. S., Sula, A., Wang, Z., Dogan, N. S., & Arvas, E. (2005, April). MICS transceivers: regulatory standards and applications [medical implant communications service]. In Proceedings. IEEE SoutheastCon, 2005. (pp. 179-182). IEEE.

[36] Patel, M., & Wang, J. (2010). Applications, challenges, and prospective in emerging body area networking technologies. IEEE Wireless communications, 17(1), 80-88.

[37] Pushpalatha, M. S., Kayalvizhi, S., Nansi, N. M. D., & Kumar, D. N. (2016). A Survey on Breast Cancer Detection Techniques. International Journal of Computer Science and Information Technologies, 7(6), 2445-2447.

[38] Heywang-Köbrunner, S. H., Hacker, A., & Sedlacek, S. (2011). Advantages and disadvantages of mammography screening. Breast care, 6(3), 199-207.

[39] Waks, A. G., & Winer, E. P. (2019). Breast cancer treatment. Jama, 321(3), 316-316.

[40]https://www.breastcancer.org/pathology-report/breast-cancer stages#articleEndAdvisors.

[41] Sheoran, G., & Kumari, V. (2019). Anatomically Real Microwave Tissue Phantoms. In Biomedical Engineering and its Applications in Healthcare (pp. 43-63). Springer, Singapore.

[42] Ito, K. (2007, November). Human body phantoms for evaluation of wearable and implantable antennas. In The Second European Conference on Antennas and Propagation, EuCAP 2007 (pp. 1-6). IET.

[43] Lazebnik, M., Madsen, E. L., Frank, G. R., & Hagness, S. C. (2005). Tissue-mimicking phantom materials for narrowband and ultrawideband microwave applications. Physics in Medicine & Biology, 50(18), 4245.

[44] Joachimowicz, N., Conessa, C., Henriksson, T., & Duchêne, B. (2014). Breast phantoms for microwave imaging. IEEE Antennas and Wireless Propagation Letters, 13, 1333-1336.

[45] Henriksson, T., Joachimowicz, N., Conessa, C., & Bolomey, J. C. (2010). Quantitative microwave imaging for breast cancer detection using a planar 2.45 GHz system. IEEE Transactions on Instrumentation and Measurement, 59(10), 2691-2699.

[46] Fiaschetti, G., Browne, J. E., Cavagnaro, M., Farina, L., & Ruvio, G. (2018, May). Tissue mimicking materials for multi-modality breast phantoms. In 2018 2nd URSI Atlantic Radio Science Meeting (AT-RASC) (pp. 1-6). IEEE.

[47] Oliveira, B., Jones, E., Glavin, M., & O'Halloran, M. (2018). Towards improved breast cancer detection using microwave technology and machine learning (Doctoral dissertation, Ph. D. thesis, NUI Galway).

[48] Porter, E., Fakhoury, J., Oprisor, R., Coates, M., & Popović, M. (2010, April). Improved tissue phantoms for experimental validation of microwave breast cancer detection. In Proceedings of the fourth European conference on antennas and propagation (pp. 1-5). IEEE.

[49] Croteau, J., Sill, J., Williams, T., & Fear, E. (2009, February). Phantoms for testing radar-based microwave breast imaging. In 2009 13th International Symposium on Antenna Technology and Applied Electromagnetics and the Canadian Radio Science Meeting (pp. 1-4). IEEE.

[50] Hahn, C., & Noghanian, S. (2012). Heterogeneous breast phantom development for microwave imaging using regression models. International journal of biomedical imaging, 2012.

[51] Singh, I., & Tripathi, V. S. (2011). Micro strip patch antenna and its applications: a survey. Int. J. Comp. Tech. Appl, 2(5), 1595-1599..

[52] Thatere, A., & Zade, P. L. (2020). Defected ground structure microstrip antenna for WiMAX. In Optical and Wireless Technologies (pp. 333-346). Springer, Singapore.

[53] Varshney, H. K., Kumar, M., Jaiswal, A. K., Saxena, R., & Jaiswal, K. (2014). A survey on different feeding techniques of rectangular microstrip patch antenna. International Journal of Current Engineering and Technology, 4(3), 418-423.

[54] Ortega-Palacios, R., Leija, L., Vera, A., & Cepeda, M. F. J. (2010, September). Measurement of breast-tumor phantom dielectric properties for microwave breast cancer treatment evaluation. In 2010 7th International conference on electrical engineering computing science and automatic control (pp. 216-219). IEEE.

[55] Kumari, V., Sheoran, G., & Kanumuri, T. (2020). SAR analysis of directive antenna on anatomically real breast phantoms for microwave holography. Microwave and Optical Technology Letters, 62(1), 466-473.

[56] Seabury, D. (2005). An update on SAR standards and the basic requirements for SAR assessment. Feature Article, Conformity, 1-8.

[57] Hopp, T., Ruiter, N., Bamber, J. C., Duric, N., & Dongen, K. W. A. (2017). Procceding of Inernational Workshop on Medical Ultrasound Tomography. Speyer Germany.

# APPENDIX

## Antenna Design

This appendix is devoted to design step of the antenna used in this study. First of all, a traditional antenna which resonates at 2.4 GHz was designed according to the values in table A.1 and illustrated in Figure A.1. The S11 value of the designed antenna was -30.86 dB.

Table A.1: Traditional antenna parameters

| Parameters | Dimensions (mm) |
|---|---|
| Patch Width (Wp) | 29.58 |
| Patch Length (Lp) | 29.58 |
| Substrate/Ground Width (Ws) | 38 |
| Substrate/Ground Length (Ls) | 38 |
| Thickness of Patch / Ground (t) | 0.035 |
| Thickness of Substrate (h) | 1.6 |
| Feedline Width (Wf) | 3.05 |
| Inset Length (d) | 9 |
| Gap (g) | 1 |

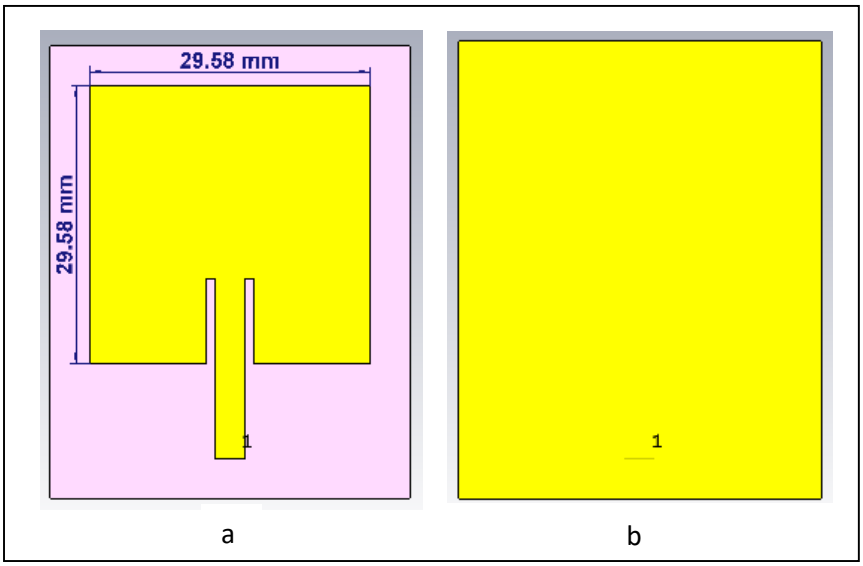


Figure A.1: Traditional antenna design.
(a) Front view, (b) Back view

The final structure of the antenna is obtained after six stages. The evolution of the proposed antenna for the first five stages are shown in Figure A.2. In the first stage, a section in the shape of a square is subtracted at the top middle section of the traditional antenna, as shown in Figure A.2a. The antenna showed resonation at 2.45 GHz with a reflection coefficient of -27 dB. In this case, modifications have been made to the design in order to both set the frequency to 2.4 GHz and increase the impedance matching. Long rectangular structures are then subtracted with two sides to shift the resonant frequency as shown in Figure A.2b. After this evaluation at the stage 2, it has been observed that the addition of comb sections allows the frequency to approach 2.4 GHz. For this reason, the number of comb protrusions was increased in the third stage (shown in Figure A.2c). While waiting for the frequency to approach 2.4 GHz, an increase in impedance matching was observed and no change in frequency was observed. Different discontinuities were created to shift the frequency. At the fourth stage two square structures with 2x2 $mm^2$ in size was placed at the left middle part and subtracted from the antenna. Creating the discontinuities at the left side as shown in Figure A.2d, shifted the frequency to 2.41 GHz. Thus, at the fifth stage the same discontinuities were added to the right middle side and the frequency was shifted exactly to 2.4 GHz (shown in Figure A.2e). After the fifth stage the antenna resonated at 2.4 GHz with a reflection coefficient of -39 dB. The reflection coefficient characteristics and frequency change of each five stages in evolution were depicted in Figure A.3.

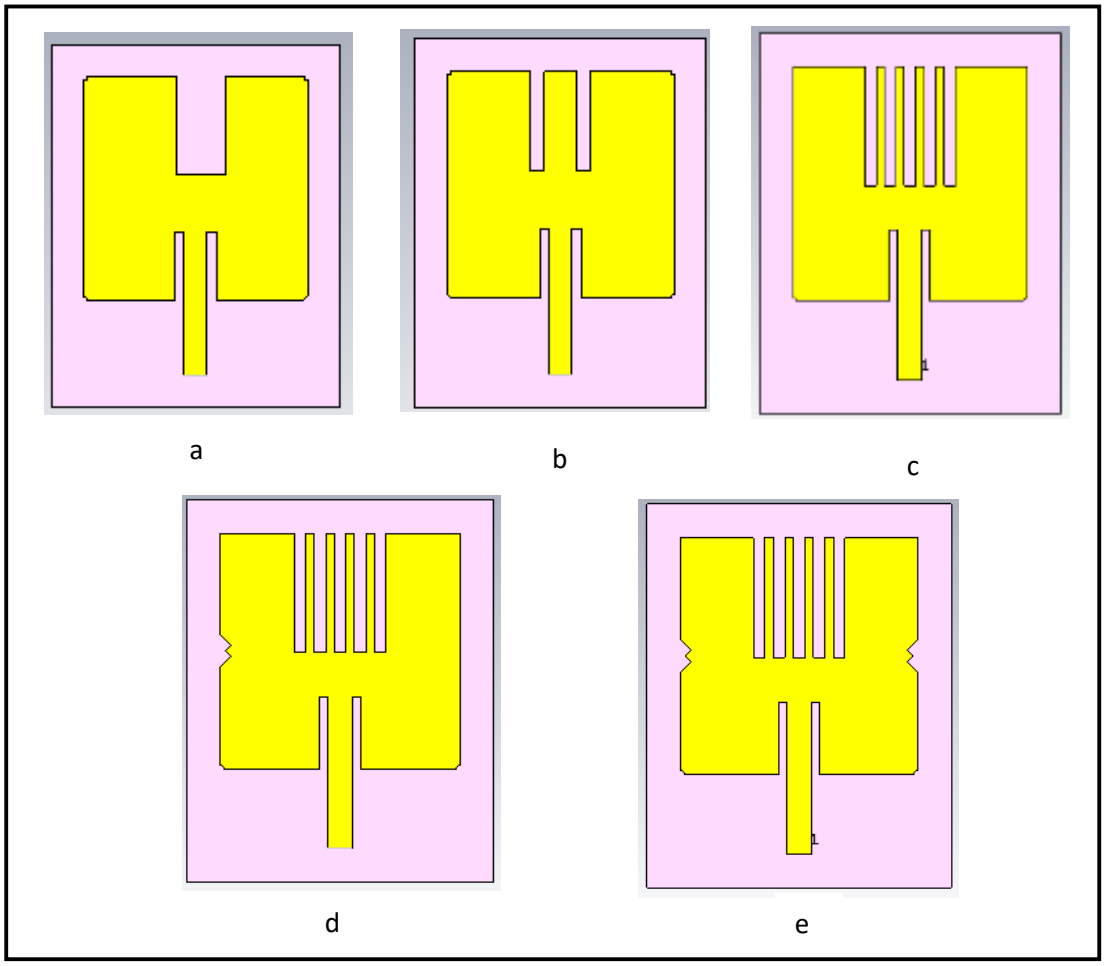


Figure A.2: Modification steps of the antenna design.
(a) Step 1, (b) Step 2, (c) Step 3, (d) Step 4, (e) Step5

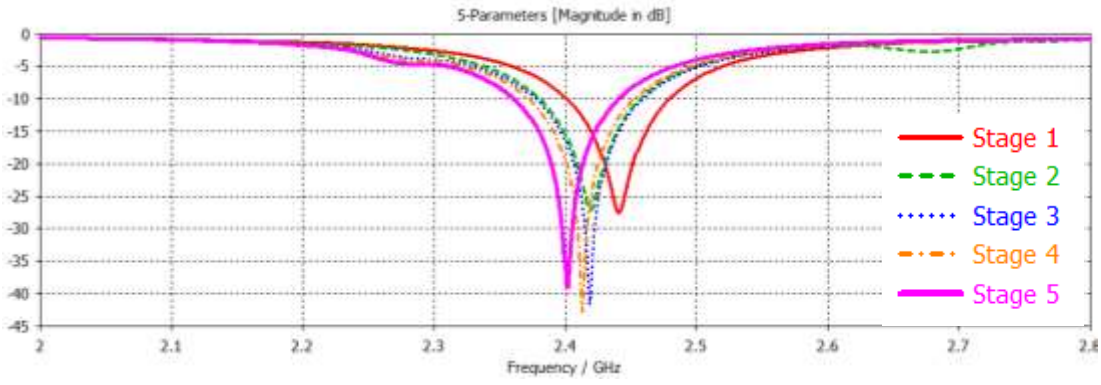


Figure A.3: Simulated return loss values of the antenna during the modification steps

After five stage evolution the antenna was placed on the healthy breast phantom and as shown in the Figure A.4, it is observed that the frequency was shifted to 2.32 GHz with a reflection coefficient of -24 dB.

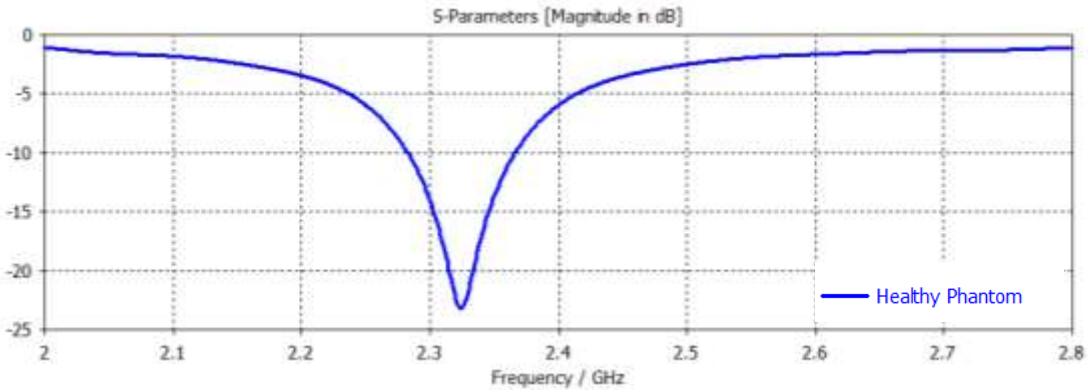


Figure A.4: Simulated return loss values of the antenna on the healthy breast phantom after 5 stage modifications

As a result of the simulations taken on the healthy breast phantom, it was decided that the antenna should be modified again due to the decrease in the frequency. Thus, in step 6, patch width, patch length and inset gap values were changed in order for the antenna to operate at 2.4 GHz on the healthy breast phantom. The length and width of the antenna was changed to 40.4 mm, 39.4 mm and 28.8 mm respectively and the inset gap was changed from 1 mm to 0.85 mm. The effect of the change on the reflection coefficient and the frequency was illustrated in Figure A.5. As a result, it is clear that 28.8 x 28.8 $mm^2$ patch antenna is the best one.

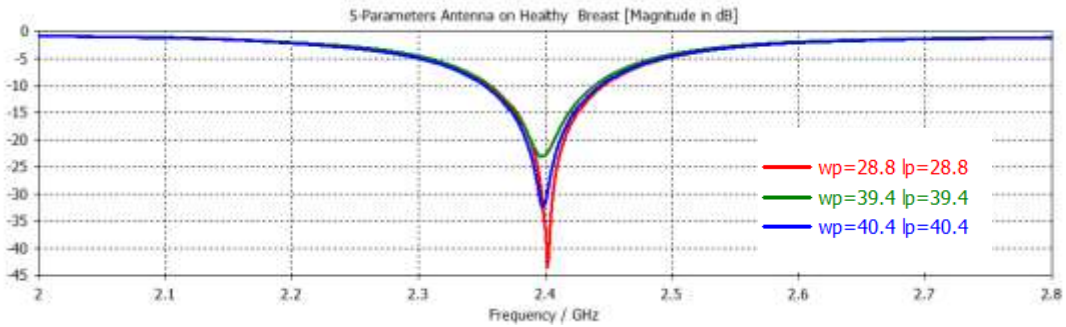


Figure A.5: Simulated return loss values of the antenna with different width and length on healthy breast phantom to adjust the frequency at 2.4 GHz